PHYSICAL REVIEW B VOLUME 28, NUMBER 2 15 JULY 1983

Bond-orientational order in liquids and glasses

Paul J. Steinhardt*
IBM Thomas J. Watson Research Center, Yorktown Heights, New York 10598

David R. Nelson
Lyman Laboratory of Physics, Harvard University, Cambridge, Massachusetts 02138

Marco Ronchetti†
IBM Thomas J. Watson Research Center, Yorktown Heights, New York 10598
(Received 27 December 1982)

Bond-orientational order in molecular-dynamics simulations of supercooled liquids and in models of metallic glasses is studied. Quadratic and third-order invariants formed from bond spherical harmonics allow quantitative measures of cluster symmetries in these systems. A state with short-range translational order, but extended correlations in the orientations of particle clusters, starts to develop about 10% below the equilibrium melting temperature in a supercooled Lennard-Jones liquid. The order is predominantly icosahedral, although there is also a cubic component which we attribute to the periodic boundary conditions. Results are obtained for liquids cooled in an icosahedral pair potential as well. Only a modest amount of orientational order appears in a relaxed Finney dense-random-packing model. In contrast, we find essentially perfect icosahedral bond correlations in alternative "amorphon" cluster models of glass structure.

I. INTRODUCTION

Two distinct broken symmetries distinguish crystalline solids from isotropic liquids. Broken translational invariance is measured by the phase of the periodic density modulations in a solid. A broken rotational symmetry is defined by the singled-out crystallographic axes. These two symmetries are not independent, because rotating one patch of perfect crystal relative to another clearly disrupts not only orientational correlations, but translational correlations as well. A relative *translation* of the two patches, on the other hand, decorrelates translational order, but leaves orientational correlations intact. It is possible to imagine states of matter with extended correlations in the orientations of locally-defined crystallographic axes, but with short-range translational order. In equilibrium, such materials would be anisotropic fluids, rather like nematic liquid crystals.[1] In contrast to conventional liquid crystals, however, the orientational anisotropy refers to the "bonds" joining near-neighbor atoms, rather than an anisotropy in the constituent particles.

Anisotropic fluids of this kind are an integral part of recent theories of two-dimensional melting[2,3] based on a dislocation mechanism proposed by Kosterlitz and Thouless.[4,5] There are indications of quenched analogs of these anisotropic fluids, with sixfold "hexatic" bond-orientational order, in two-dimensional binary mixtures at low temperatures.[6] It is natural to inquire about three-dimensional bond-orientational order in simple fluids, like liquid argon, and in relatively simple disordered solids, like metallic glasses.[7] The importance of local orientational symmetries in three dimensions was emphasized over thirty years ago, in an important paper by Frank.[8] Measurements of radial distribution functions (RDF) in dense liquids indicate that each atom has roughly 12 particles in its first coordination shell. Obvious "crystallographic" clusters of 12 atoms around a central particle are shown in Figs. 1(a) and 1(b), corresponding to nuclei of fcc and hcp crystals. As observed by Frank, the icosahedral arrangement shown in Fig. 1(c) actually has a significantly lower energy, at least for simple Lennard-Jones pair potentials.[9] Frank argued that the experimentally observed ability to supercool simple liquid metals well below the equilibrium melting temperature[10] was due to the prevalence of these icosahedral clusters.

Hoare and collaborators[11] and also Farges *et al.*[12] have made extensive studies of the energetics of particle clusters, and found that noncrystallographic arrangements (like the icosahedron) are preferred over, say, an fcc cluster, until one gets to clusters of several hundred atoms. "Magic numbers" observed in molecular-beam experiments on argon[13] also suggest that crystallographic symmetries are unlikely in

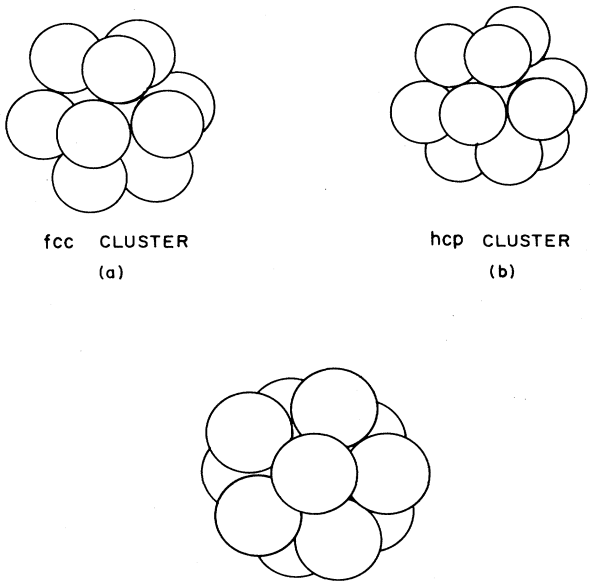

FIG. 1. Different 13-atom particle clusters occurring in liquids near the melting temperature.

small clumps of particles. Hoare has speculated that the size of these "amorphons" will grow with decreasing temperature in supercooled liquids, until limited near the glass transition by frustration effects.[11] He has also criticized traditional dense-random-packing models of metallic glasses,[14] on the grounds that the energetic preference for noncrystallographic clusters is not properly taken into account. He suggests that more realistic models of glasses can be obtained from simulations of glass formation in a soft potential without periodic boundary conditions.

In this paper, we develop ways of measuring both local and extended orientational symmetries in computer-generated models of dense liquids and glasses. Our analysis starts by associating a set of spherical harmonics with every bond joining an atom to its near neighbors. By "bonds" we of course do not mean chemical bonds, but rather lines resulting from some convenient assignation of near neighbors (see Sec. II). With a bond whose midpoint is at $\vec{r}$ we associate the set of numbers,

$$Q_{lm}(\vec{r}) \equiv Y_{lm}(\theta(\vec{r}),\phi(\vec{r})) , \tag{1.1}$$

where the $\{Y_{lm}(\theta,\phi)\}$ are spherical harmonics, and $\theta(\vec{r})$ and $\phi(\vec{r})$ are the polar angles of the bond measured with respect to some reference coordinate system. We need not associate a *direction* with a particular bond, provided our attention is restricted to even-l spherical harmonics, which are invariant under inversion. The orientational order parameters $\{Q_{lm}(\vec{r})\}$ are a natural generalization of the two-dimensional hexatic order parameter discussed in Ref. 2. As we shall see, they will allow us to determine the range of orientational order in various systems, and to study the orientational polymorphism stressed by Frank.[8] (Orientational polymorphism is not an issue in *two* dimensions, because there is essentially only one way of packing six disks around a central one.) A preliminary account of our investigations appeared in Ref. 15.

Three-dimensional bond-orientational order has been studied theoretically by Nelson and Toner,[16] who showed that simple crystalline solids disordered by an equilibrium concentration of unbound dislocation loops retain long-range *cubic* orientational order. Such materials are not isotropic liquids, as assumed in most theories of dislocation melting.[17] It was argued that supercooled liquids might drop into a phase with cubic orientational order prior to the glass transition. The possibility of extended *icosahedral* bond order (see below) was not considered. Toner[18] has discussed bond-oriented liquids with uniaxial symmetry. The onset of cubic bond-orientational order in crystals near the melting transition has been studied by Hess[19] and by Mitus and Patashinskii.[20]

In our numerical studies, we shall often consider averaged quantities, like

$$\bar{Q}_{lm} \equiv \langle Q_{lm}(\vec{r}) \rangle , \tag{1.2}$$

where the average is taken over some suitable set of bonds in the sample. The first nonzero averages (other than Q_{00}) occur for $l=4$ in samples with cubic symmetry and for $l=6$ in icosahedrally oriented systems (see Sec. II). Because the Q_{lm}'s for a given l can be scrambled drastically by changing to a rotated coordinate system, it is important to consider rotationally invariant combinations, such as

$$Q_l \equiv \left[\frac{4\pi}{2l+1} \sum_{m=-l}^{l} | \bar{Q}_{lm} |^2 \right]^{1/2} \tag{1.3}$$

and

$$W_l \equiv \sum_{\substack{m_1,m_2,m_3 \\ m_1+m_2+m_3=0}} \begin{pmatrix} l & l & l \\ m_1 & m_2 & m_3 \end{pmatrix} \times \bar{Q}_{lm_1} \bar{Q}_{lm_2} \bar{Q}_{lm_3} . \tag{1.4}$$

The coefficients

$$\begin{pmatrix} l & l & l \\ m_1 & m_2 & m_3 \end{pmatrix}$$

in the third-order invariants (1.4) are Wigner $3j$ sym-

bols.[21] We have found that the $\{Q_l\}$ and $\{W_l\}$ are the key to a kind of cluster "shape spectroscopy" in liquids and glasses. The ratios

$$\hat{W}_l \equiv W_l \Big/ \left[\sum_{l=-m}^{m} | \bar{Q}_{lm} |^2 \right]^{3/2} , \tag{1.5}$$

in particular, are a sensitive measure of the different orientational symmetries enumerated by Frank.

Many of our results refer to orientational order in a molecular-dynamics simulation of 864 atoms, subject to periodic boundary conditions, and interacting via a Lennard-Jones pair potential. In an isotropic liquid, we would expect that all $Q_{lm}(\vec{r})$ except Q_{00} vanish when averaged over the sample volume. This is indeed the case for all temperatures above the equilibrium melting temperature. Upon supercooling about 10% below T_m, however, extended orientational correlations appear, with little or no increase in the translational correlation length. The symmetry of the orientational order which develops appears to be predominantly icosahedral; it is as if the icosahedral clusters discussed by Frank[8] have begun to align. Haymet[22] has solved a simple lattice model of interacting icosahedra within the mean-field approximation, and finds that they align via a first-order phase transition, as one would expect from arguments based on Landau theory.[15] Fluctuation effects, neglected in mean-field and Landau theories, can drive such transitions continuous, however.[16] Although we interpret our results in terms of an apparent orientational phase transition,[15] one can of course never be certain that this indeed is the case in simulations of small 864-particle samples. What is clear, however, is that an orientational length scale $\xi_6(T)$ increases with decreasing temperature until it greatly exceeds the translational correlation length ξ_T,

$$\xi_6 \gg \xi_T \, . \tag{1.6}$$

This inequality appears to be in force at low temperatures, with ξ_6 limited only by our small sample size. Qualitatively similar results were obtained at two different densities, and in a smaller 600-particle system.

The symmetry of the bond-oriented states we find is not perfectly icosahedral. This is probably due to the periodic boundary conditions, which favor cubic order. Another possibility is that the sample consists of several icosahedral "domains." To study this point further, we repeated our simulations using a Lennard-Jones pair potential augmented by a small direction-dependent part with an icosahedral symmetry. Upon cooling well below the apparent orientational transition, and then slowly turning off the applied icosahedral "field," we obtained a bond-oriented state with enhanced icosahedral order. These results are consistent with a picture of icosahedral domains aligned by the field-cooling process. Imposing a very strong icosahedral field generated not only icosahedral bond order, but discernable *cubic* order as well. In Sec. III F, we argue that this is due to a coupling between icosahedral order and the periodic boundary conditions. Although molecular-dynamics simulations of Lennard-Jones liquids often crystallize when supercooled,[23] we found that a small icosahedral field always suppressed crystallization.

Crystallization before significant supercooling can take place makes experimental studies of real Lennard-Jones liquids like argon rather difficult. Studies via the molecular-dynamics technique are possible because of the extremely limited maximum-run times ($\sim 10^{-9}$ sec in argonlike units) available even with very-high-speed computers. It would be interesting to search for bond order in liquid metals, however, since these materials can be significantly undercooled in the laboratory.[10] Our results also have implications for metallic glasses, which might conceivably have frozen-in bond-orientational order. Crystallization is suppressed in metallic glasses by rapid quenching, and by using materials with at least two different components.[7]

We have searched for frozen-in bond order in a number of simple models of glasses. Weak but persistent orientational order appears in a relaxed 3701-atom portion of the Finney model[24] of dense random packing. We have also computed the spherical harmonics for a spiral configuration of "twisted tetrahedra" discussed by Bernal.[25] Bernal argued that these linear structures could be found throughout his random packing models of dense liquids. The average spherical harmonics are small, but presumably would be much larger if the order-parameter equation (1.2) is averaged with a spatially dependent rotation that matches the pitch of the Bernal spiral. This sort of order if it occurred in bulk systems would be a kind of bond-oriented analog of a cholesteric liquid crystal.[1]

Exceptionally strong orientational order appears in some of the noncrystallographic clusters discussed by Hoare. In addition to the 13-atom simple icosahedron, we have studied a 43-atom "icosadodecahedron," and a 127-atom "rhombicosadodecahedron." When these clusters are relaxed, we find essentially perfect icosahedral bond-orientational order. It is remarkable that the spherical harmonics of the 324 bonds of the icosadodecahedron and the 1212 bonds of the rhombicosadodecahedron add so coherently; these clusters exhibit only weak bond order before relaxation, even though their overall rotational symmetry appears icosahedral.

In view of these results, it is tempting to associate the orientational correlation length $\xi_6(T)$ we find in Lennard-Jonesium with the size of the "amorphons" discussed by Hoare.[11] Of course, the correlations we measure are statistical averages over all bond angles; literal icosahedral clusters are not required. It is interesting that the increase in $\xi_6(T)$ seems to come well above the molecular-dynamics glass "transition" temperature T_g.[23] Hoare suggested a large increase in the amorphon size close to T_g.[11]

Extended bond-orientational order, when it exists at all in real materials,[26] is an extremely subtle effect. An icosahedron, after all, is a rather good approximation to an isotropic sphere. Because the broken symmetry is typically higher than uniaxial ($l \geq 4$), most bond-oriented materials (in contrast to nematic liquid crystals) would not be optically active. As discussed in Sec. II, the structure function $S(\vec{q})$ in bond-oriented liquids and glasses should have a directional modulation reflecting the broken orientational symmetry. Alben *et al.*[27] have, in fact, found an interesting direction dependence in $S(\vec{q})$ for a 996-atom relaxed Finney model. Their results seem consistent with our observation of weak orientational order in this system. All evidence of bond-orientational order would, of course, be lost in a directionally-averaged "powder" x-ray diffraction pattern.

Local orientational order could be measured by focusing down an x-ray beam until it illuminates a very small sample volume (say 100 atoms), and then observing the directional modulations in $S(\vec{q})$. This experiment has already been done via light scattering in films of polystyrene spheres, suspended in water between two glass plates.[28] The interparticle spacing is several thousand angstroms, and so light diffracts as x rays would in conventional materials. Bulk colloidal "glass" phases in binary suspensions[29] could also be studied in this way. By cross-correlating data from two small sample volumes, the orientational correlation length could be measured directly. Time autocorrelation functions in liquids would also be interesting, since the onset of long-range orientational order in space should be accompanied by extended temporal correlations as well.

A number of indirect manifestations of bond order are possible: (1) Liquids which drop into icosahedrally oriented phases upon supercooling should be exceptionally resistant to crystallization. There should be a pronounced asymmetry in the limits of superheating and supercooling, in such materials as suggested previously in the case of cubic bond order.[16] It is even possible that some liquid metals drop into an icosahedral phase above the equilibrium melting temperature. (2) The very different translational and orientational length scales present in an oriented fluid may play a role in glass formation. Vogel-Fulcher fits to the viscosity of glass-forming liquids must be redone at temperatures such that η reaches $10^4 - 10^6$ P.[30] Perhaps this temperature is associated with an anomaly in the orientational order. (3) Magnetic metallic glasses exhibit particularly "soft" hysteresis loops, as one might expect in an amorphous material.[7] The small *residual* hysteresis observed experimentally is often attributed to frozen-in strains. Another explanation would be frozen-in orientational order, which would act in many ways like a small crystal field on the magnetization.

In Sec. II, we discuss how to measure bond-orientational order in simple cases. A number of useful theoretical ideas are tabulated in Sec. III. In Sec. IV, molecular-dynamics simulations of Lennard-Jones particles are described. Orientational order in models of amorphous materials is discussed in Sec. V. In Sec. VI, we conclude with comments on the nature of an icosahedrally oriented liquid and its possible relevance to the glass transition.

II. MEASURING BOND-ORIENTATIONAL ORDER

In order to evaluate the bond-orientational order parameter (1.2), we must first define what is meant by a "near neighbor." We have found it computationally convenient to consider all atoms within $1.2r_0$ of a given particle as near neighbors, where r_0 is, say, the minimum in a Lennard-Jones potential. More generally, one could take r_0 to be the position of the first peak in the radial distribution function. This definition insures that all atoms in the first coordination shell are counted as near neighbors, which is the definition used by Frank.[8] Average bond order parameters can then be evaluated by summing over all bonds in the sample,

$$\bar{Q}_{lm} = \frac{1}{N_b} \sum_{\text{bonds}} Q_{lm}(\vec{r}) , \tag{2.1}$$

where N_b is the number of bonds.

Another common definition of near neighbors proceeds via the construction of Voronoi polyhedra.[31] Each face of every polyhedron bisects a near-neighbor bond. With this definition, one might want to weight the $Q_{lm}(\vec{r})$ by the solid angle subtended by the face of the corresponding Voronoi polyhedron so that distant near neighbors are deemphasized relative to closer ones. We have found no changes in our basic results upon changing the definition of near neighbor. For example, all reasonable definitions lead to $\bar{Q}_{lm}$ which vanish in isotropic liquids for $l > 0$, and which are nonzero in cubic solids for $l \geq 4$. The quantity $\bar{Q}_{00}$ (corresponding to the constant spherical harmonic

$Y_{00}=1/\sqrt{4\pi}$) is always nonzero, and scales with the average coordination number associated with a particular convention for assigning neighbors.

A number of earlier studies of symmetries in liquids and dense-random-packing models have been reviewed by Collins.[31] Most of these investigations catalog the number of faces, edges, and vertices of Voronoi polyhedra. The angular distribution of neighbors in the first three coordination shells for hard-sphere random close packing has been calculated by Scott and Mader.[32] This work focuses on the angles *between* bonds in the various coordination shells. The bond angles entering in Eq. (1.3) are different, because they are measured with respect to an external coordinate system. We shall see, however, that the $Q_{lm}(\vec{r})$ are a sensitive measure of the kind of features studied by Scott and Mader.[32]

The spherical harmonics $Y_{lm}(\theta,\phi)$ for a given value of l (and $|m| \leq l$) form a $(2l+1)$-dimensional representation of the rotational group SO(3). This means that the $Q_{lm}(\vec{r})$ corresponding to a particular representation are scrambled by rotating the external coordinate system. To eliminate the dependence on the arbitrary orientation of the external reference axes, one must form the invariants (1.3) and (1.4) defined in the Introduction. Figure 2 shows these invariants for five different bond clusters, and $l=2$, 4, 6, 8, and 10. The averages are over the 12 bonds emanating from the central particle in the icosahedral, fcc, and hcp clusters shown in Fig. 1, and correspond to 14 and 6 such bonds, respectively, in bcc and simple cubic (sc) clusters. Note that nonzero averages appear for $l \geq 4$ in the hcp cluster and in the clusters with cubic symmetry (fcc, bcc, and sc). Identical results would be obtained for infinite fcc, bcc, and sc crystals, since our clusters corresond to unit cells. In general one would expect a signal at $l=2$ in infinite hcp crystals. The $l=2$ component vanishes accidentally, however, for the 13-atom hcp cluster corresponding to close packing of hard spheres.

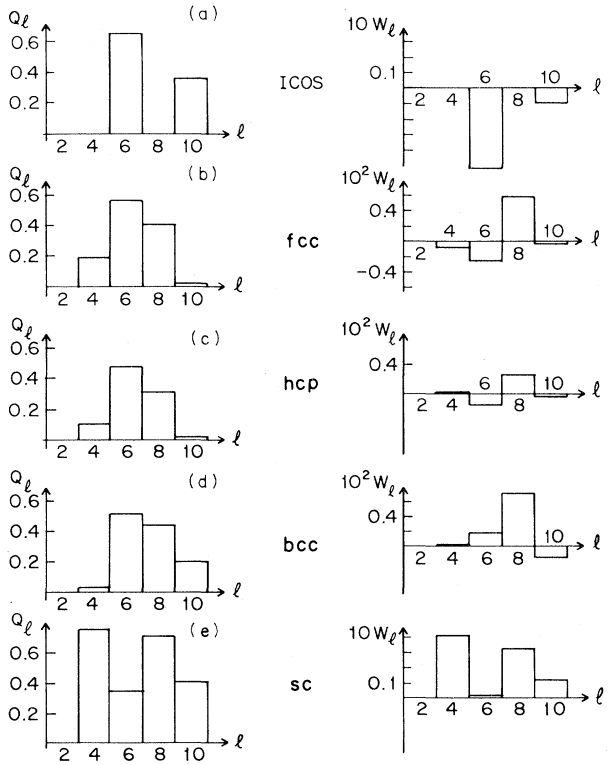

FIG. 2. Histograms of quadratic and third-order invariants for 13-atom icosahedral, fcc, and hcp clusters, as well as for 15-atom bcc and 7-atom sc clusters. Bonds at the surface are excluded.

Note that nonzero averages occur only at $l=6$ and 10 for the icosahedral cluster. More generally, clusters with an icosahedral symmetry can have nonzero spherical harmonics only for $l=6,10,12,\ldots$.[33] The particular values of l for which nonzero spherical harmonics can occur depend only on the cluster symmetry. The *magnitudes* of the nonzero $\{Q_l\}$ and $\{W_l\}$, however, can be changed by altering the definition of near neighbor, and by including surface bonds in the average.

It is useful to have a more quantitative measure of the symmetry of a cluster, namely

$$\hat{W}_l \equiv \frac{\sum_{\substack{m_1,m_2,m_3 \\ m_1+m_2+m_3=0}} \begin{pmatrix} l & l & l \\ m_1 & m_2 & m_3 \end{pmatrix} Q_{lm_1} Q_{lm_2} Q_{lm_3}}{\left[\sum_m |Q_{lm}|^2\right]^{3/2}} . \tag{2.2}$$

This quantity is normalized so that it is independent of the overall magnitude of the $\{Q_{lm}\}$ for a given l. The remarkable sensitivity of the $\{\hat{W}_l\}$ to cluster symmetries is illustrated in Table I, which shows these quantities for the five clusters tabulated in Fig. 2. Despite their rather different Q_l and W_l histograms, the cubic fcc, bcc, and sc clusters have identical $\hat{W}_l$'s, except for a sign. Although the signs can change, the magnitudes of the $\hat{W}_l$'s are unaffected by including surface bonds in the averages and by changing the definition of nearest neighbor.

The parameters $|\hat{W}_l|$ are a direct index of the symmetry of a particular cluster (see Sec. III). Specifying the Q_{lm}'s in a standard coordinate system leads to a closely related measure of symmetry. Consider for concreteness the 14 bonds piercing the faces of the Wigner-Seitz cell of a bcc crystal. In a coordinate system aligned with the cubic unit cell, all spherical harmonics except Y_{40} and $Y_{4\pm4}$ vanish

TABLE I. Reduced invariants $\hat{W}_l$, calculated numerically, for the simple shapes whose quadratic and third-order invariants are cataloged in Fig. 2.

	$\hat{W}_4$	$\hat{W}_6$	$\hat{W}_8$	$\hat{W}_{10}$
icos		−0.169 754		−0.093 967
fcc	−0.159 316	−0.013 161	+0.058 454	−0.090 128
hcp	+0.134 097	−0.012 442	+0.051 259	−0.079 854
bcc	+0.159 317	+0.013 161	−0.058 455	−0.090 130
sc	+0.159 317	+0.013 161	+0.058 455	+0.090 130

when averaged as in Eq. (2.1). It is straightforward to check that the six bonds along the cubic axes give a contribution

$$\sum_{\text{axes}} Q_{40}(\vec{r}) = \left[\frac{9}{4\pi}\right]^{1/2} \frac{7}{2} = (\tfrac{14}{5})^{1/2} \sum_{\text{axes}} Q_{4\pm4}(\vec{r}) , \tag{2.3a}$$

while the eight bonds along the cube diagonals give

$$\sum_{\text{diag}} Q_{40}(\vec{r}) = \left[\frac{9}{4\pi}\right]^{1/2} \frac{28}{9} = (\tfrac{14}{5})^{1/2} \sum_{\text{diag}} Q_{4\pm4}(\vec{r}) . \tag{2.3b}$$

Although the signs and numerical magnitudes differ, note that the ratio of the Q_{40} sum to the $Q_{4\pm4}$ sum is $(\frac{14}{5})^{1/2}$ in each case. This signature of cubic symmetry is preserved no matter how we weight the relative contributions of (2.3a) and (2.3b) to averages like (2.1). In Sec. III, we shall see that bond order parameters such that

$$\bar{Q}_{40}^2 = \tfrac{14}{5} \, | \, \bar{Q}_{4\pm4} \, |^2 \tag{2.4}$$

with all other $\bar{Q}_{4m}=0$ maximize $| \hat{W}_4 |$.[34,35] Note that $\bar{Q}_{40}$ is positive for the bonds represented in Eq. (2.3a) and negative for the "dual" bonds summed in Eq. (2.3b). It turns out that the sign of $\bar{Q}_{40}$ determines the sign of W_4 for cubic clusters in this special coordinate system. One can imagine situations in which the $\bar{Q}_{4m}$ are "accidentally" small for clusters with cubic symmetry due to cancellations.

Similar results hold for icosahedral clusters. In a coordinate system such that all $\bar{Q}_{6m}$ vanish except $\bar{Q}_{60}$ and $\bar{Q}_{6\pm5}$, one always finds that

$$\bar{Q}_{60}^2 = \tfrac{11}{7} \, | \, \bar{Q}_{6\pm5} \, |^2 . \tag{2.5}$$

This set of order parameters is an extremum which very likely maximizes $| \hat{W}_6 |$.[34] The sign of $\hat{W}_6$ is determined by the sign of $\bar{Q}_{60}$. The quantity $\bar{Q}_{60}$ is positive for the 12 bonds of a simple icosahedron, and negative for the dual bonds at the vertices of a dodecahedron.

Given an arbitrary cluster of atoms, one can see how nearly cubic or icosahedral it is by evaluating the $| \hat{W}_l |$ and comparing with the entries in Table I. Since $\hat{W}_4$ is undefined for icosahedra, the comparison is best made at $l=6$, where one typically finds a strong signal (see Fig. 2). It turns out that the cubic $l=6$ order parameters are also an extremum of $| \hat{W}_6 |$, but with a value about 12.9 times smaller than the icosahedral one.[34] The hcp cluster gives a $| \hat{W}_6 |$ which is close to the cubic value, although the $\hat{W}_4$'s are rather different. The sensitive dependence of the $\hat{W}_l$ on cluster symmetries is very helpful in studying the orientational polymorphism discussed in the Introduction.

One can always analyze a cluster by trying to find a special coordinate system in which its spherical harmonics simplify. To do this, we use the relation[36]

$$\bar{Q}'_{6m} = \sum_{m'} D^{(6)}_{m,m'}(\alpha,\beta,\gamma) \bar{Q}_{6m} , \tag{2.6}$$

which shows how spherical harmonics transform when the coordinate system is rotated with Euler angles α, β, and γ. The Wigner matrices $D^{(l)}_{m,m'}$ form a $(2l+1)$-dimensional representation of the rotational group. To identify nearly icosahedral clusters, for example, one would first search for Euler angles such that all Q'_{6m} except Q'_{60} and $Q'_{6\pm5}$ equal zero, and then see how well (2.5) is obeyed. Although this procedure is more tedious than simply evaluating $| \hat{W}_6 |$, it can give interesting information about the preferred coordinate system. The icosahedral order we found in supercooled "Lennard-Jonesium," for example, was often aligned by the periodic boundary conditions (see Sec. IV).

III. THEORETICAL BACKGROUND

A. Landau theory

Many of the results discussed empirically in Sec. II become more transparent when viewed in the context of Landau's general theory of phase transitions.[37] Even in systems with only short-range orientational order, the symmetry principles under-

lying Landau's approach provide useful insights.

Following Ref. 16, we start by considering a density of bonds $\rho(\Omega)$ piercing the unit sphere, as a function of solid angle $\Omega=(\theta,\phi)$. We assume that $\rho(\Omega)$ is obtained by averaging over all bonds in the system. This density can always be expanded in spherical harmonics, which form a complete set of functions on the unit sphere,

$$\rho(\Omega)=\sum_{l=0}^{\infty}\sum_{m=-l}^{l} Q_{lm}\,Y_{lm}^{*}(\Omega)\ . \tag{3.1}$$

The expansion coefficients Q_{lm} are just the bond order parameters considered in the preceding section. By counting all bonds in both of the two possible directions which can be assigned to them, we insure that all coefficients with odd l vanish. In isotropic systems, all Q_{lm} except Q_{00} are zero. A state with a broken orientational symmetry is characterized by some smallest value of $l>0$ for which $Q_{lm}\neq 0$,

$$\begin{aligned}\delta\rho(\Omega)&=\rho(\Omega)-Q_{00}/\sqrt{4\pi}\\ &=\sum_{m=-l}^{l} Q_{lm}\,Y_{lm}^{*}(\Omega)+\cdots\ ,\end{aligned} \tag{3.2}$$

where the ellipsis stands for "harmonics." The numbers Q_{lm} form a $(2l+1)$-dimensional order parameter describing the low-temperature bond-oriented phase. The higher-order terms labeled "harmonics" are usually small, and will be discussed further in the next subsection.

Landau's approach is to expand the difference between the isotropic and bond-oriented free energies F_l in rotationally invariant combinations of the first nonzero $\{Q_{lm}\}$. This expansion takes the form[38]

$$F_l=r_l\sum_{m=-l}^{l}|Q_{lm}|^2+w_l\sum_{\substack{m_1,m_2,m_3\\ m_1+m_2+m_3=0}}\begin{pmatrix} l & l & l\\ m_1 & m_2 & m_3\end{pmatrix}Q_{lm_1}Q_{lm_2}Q_{lm_3}+O(Q_{lm}^4)\ , \tag{3.3}$$

where r_l and w_l are temperature-dependent parameters. Assuming that $r_l(T)$ becomes negative with decreasing temperature, one finds that F_l is eventually minimized by a state such that

$$Q_{lm}\neq 0 \tag{3.4}$$

at low temperatures. If the third-order coupling w_l is nonzero, Landau theory predicts that the transition to this state will be first order.

The quantity

$$\left[\sum_{m=-l}^{l}|Q_{lm}|^2\right]^{1/2} \tag{3.5}$$

can be viewed as the "magnitude" of the $(2l+1)$-dimensional order parameter. For a fixed magnitude, a variety of different states are possible. If the transition is only weakly first order, the preferred state can be found by minimizing the third-order term in (3.3), with the magnitude held fixed. The problem reduces to finding extrema of the symmetry parameter $\hat{W}_l$ introduced in Sec. II. If w_l is positive, we want to minimize $\hat{W}_l$, while negative w_l means that $\hat{W}_l$ should be a maximum.

The quantity $\hat{W}_4$ was discussed for systems with cubic symmetry in Ref. 16. In a coordinate system such that only Q_{40} and $Q_{4\pm4}$ are nonzero, we have (using the $3j$ symbols tabulated, for example, in Ref. 21)

$$W_4=\frac{30(4!)^{3/2}}{\sqrt{13!}}\,\frac{3Q_{40}^3+14Q_{40}|Q_{44}|^2}{(Q_{00}^2+2|Q_{44}|^2)^{3/2}}\ , \tag{3.6a}$$

where the relation

$$Q_{4,-4}=Q_{44}^{*} \tag{3.6b}$$

has been used to eliminate $Q_{4,-4}$. It is easily shown that (3.6) is maximized when $Q_{40}>0$ and Eq. (2.4) is satisfied. The corresponding minimum occurs for $Q_{40}<0$. The problem of finding extrema of the $\{\hat{W}_l\}$ has been considered more generally by Busse[34] and Sattinger,[35] who were interested in patterns of fluid convection in spherical shells. Busse shows that the solution (2.4) is an extremum in the nine-dimensional space spanned by all possible $l=4$ spherical harmonics. He further argues on the basis of numerical evidence that this solution is a global maximum or minimum, depending on the sign of Q_{40}. Of course, a three-parameter family of equivalent solutions can be obtained by rotating the external coordinate system. Sattinger[35] has obtained the eigenvalues about the cubic extremum, and finds that they are consistent with Busse's conjecture. Inserting the relation (2.4) in (3.6), we find that, at the cubic extremum

$$\hat{W}_4^{\text{cubic}}=\tfrac{7}{3}\left(\tfrac{2}{429}\right)^{1/2}=0.159\,317\ , \tag{3.7}$$

in agreement with the values for the cubic clusters displaced in Table I.

The invariant $\hat{W}_6$ is easily minimized in an "icosahedral" subspace spanned by Q_{60} and $Q_{6\pm5}$, with all other $Q_{6m}=0$.[15] Inserting the relevant $3j$ coefficients, we find that

$$\hat{W}_6 = -420\frac{(6!)^{3/2}}{\sqrt{19!}}\frac{4Q_{60}^3 + 33Q_{60}|Q_{65}|^2}{(Q_{60}+2|Q_{65}|^2)^{3/2}} , \tag{3.8a}$$

where we have used the relation

$$Q_{6,-5} = -Q_{65}^* . \tag{3.8b}$$

Extrema of Eq. (3.8a) occur when the relation (2.5), characteristic of icosahedral clusters, is satisfied. The icosahedral value of $\hat{W}_6$ is

$$|\hat{W}_6^{\text{icos}}| = \frac{11}{\sqrt{4199}} = 0.169\,754 . \tag{3.9}$$

In the right coordinate system, cubic clusters have only Q_{60} and $Q_{6\pm4}$ nonzero. In this subspace we have

$$\hat{W}_6 = 336\frac{(6!)^{3/2}}{\sqrt{19!}}\frac{(-5Q_{60}^3 + 6Q_{60}|Q_{64}|^2)}{(Q_{60}^2+2|Q_{64}|^2)^{3/2}} , \tag{3.10}$$

which has a nontrivial extremum for

$$\frac{Q_{60}^2}{|Q_{6\pm4}|^2} = \frac{2}{7} \tag{3.11}$$

corresponding to

$$|\hat{W}_6^{\text{cubic}}| = \frac{4}{\sqrt{92\,378}} \simeq 0.013\,161 . \tag{3.12}$$

Busse[34] has shown that these two configurations are in fact extrema in the full 13-dimensional space of $l=6$ spherical harmonics, and has further speculated that $|\hat{W}_6^{\text{icos}}|$ is a global maximum of $|\hat{W}_6|$. In the extensive numerical calculations reported later in this paper, we have never found a configuration of spherical harmonics such that $|\hat{W}_6|$ exceeds (3.9), in agreement with Busse's conjecture. Note that (3.9) and (3.12) agree with the numerical results for icosahedral and cubic clusters in Table I.

Clusters with an hcp symmetry are a somewhat special case. It is natural to allow for a variable uniaxial symmetry, and consider clusters which are stretched or compressed along the z axis relative to the "hard-sphere" hcp configuration shown in Fig. 1(c). In this coordinate system, only Q_{60} and $Q_{6\pm6}$ can be nonzero, independent of the amount of distortion. The $l=6$ invariant becomes

$$\hat{W}_6 = 168\frac{(6!)^{3/2}}{\sqrt{19!}}\frac{-10Q_{60}^3 + 33Q_{60}|Q_{66}|^2}{(Q_{60}^2+2|Q_{66}|^2)^{3/2}} \tag{3.13}$$

in this hcp subspace. The extremal hcp configuration occurs for

$$\frac{Q_{60}^2}{|Q_{6\pm6}|^2} = \frac{11}{21} , \tag{3.14}$$

which gives

$$|\hat{W}_6^{\text{ext hcp}}| = \frac{22}{\sqrt{222\,547}} \simeq 0.046\,635 . \tag{3.15}$$

Figure 3 shows the quantity $\hat{W}_6$ for a 13-atom hcp cluster as a function of the stretching or compression along the z axis. Note that the minimal $\hat{W}_6$ configuration does not correspond to the hard-sphere configuration shown in Fig. 1(c) $[(\frac{3}{8})^{1/2}c/a=1]$ which is only a local maximum. The results (3.14) and (3.15) correspond to another extremal $l=6$ configuration found by Busse.[34] Note that (3.15) is still rather far from the icosahedral value of $\hat{W}_6$. A general hcp cluster will also have nonzero $l=4$ spherical harmonics. In the coordinate system discussed above, it is easily shown that only Q_{40} is nonzero, and that

$$|\hat{W}_4^{\text{hcp}}| = \begin{vmatrix} 4 & 4 & 4 \\ 0 & 0 & 0 \end{vmatrix} = \frac{90(4!)^{3/2}}{\sqrt{13!}} \simeq 0.134\,097 . \tag{3.16}$$

There is also a "uniaxial" extremum with only $Q_{60}\neq0$, and

$$|\hat{W}_6^{\text{uniax}}| = \begin{vmatrix} 6 & 6 & 6 \\ 0 & 0 & 0 \end{vmatrix} = \frac{-1680(6!)^{3/2}}{\sqrt{19!}} \approx -0.093\,060 . \tag{3.17}$$

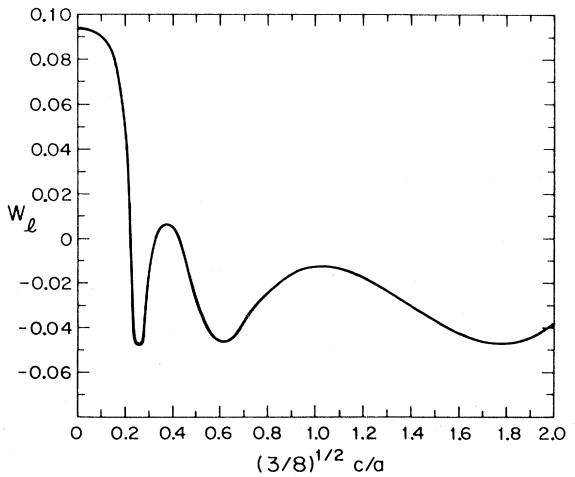

FIG. 3. Symmetry parameter $\hat{W}_6$ for a 13-atom hcp cluster as a function of aspect ratio c/a. The two equilateral triangles above and below the "equatorial plane" of Fig. 1(b) have been stretched along the c axis. The c/a ratio corresponding to hard spheres is $(\frac{8}{3})^{1/2}$.

Transitions to orientationally ordered states need not be first order, notwithstanding predictions based on Landau theory. As shown in Ref. 16 for the case of cubic order, fluctuation effects, neglected in Landau's approach, drive the transition continuous in $2+\epsilon$ dimensions. Similar conclusions apply for icosahedral transitions, and for the case $l=2$ describing nematic liquid crystals.[16] It is hard to say what happens in three dimensions. The experimentally observed isotropic-to-nematic transition is first order, but much weaker than one would expect based on mean-field and Landau theories.[1]

B. Coupling between order parameters and effect of periodic boundary conditions

Landau theory also provides a convenient way of determining which of the terms labeled "harmonics" in Eq. (3.2) are nonzero, and allows a discussion of the coupling between different spherical harmonics in general. Suppose we are interested in the interplay between $l=4$ and $l=6$ spherical harmonics. The most general free energy to third order in the Q_{lm} is

$$F=F_4+F_6+w_{6,4}\sum_{\substack{m_1,m_2,m_3\\ m_1+m_2+m_3=0}}\begin{bmatrix}6&6&4\\ m_1&m_2&m_3\end{bmatrix}Q_{6m_1}Q_{6m_2}Q_{4m_3}$$
$$+w_{4,6}\sum_{\substack{m_1,m_2,m_3\\ m_1+m_2+m_3=0}}\begin{bmatrix}4&4&6\\ m_1&m_2&m_3\end{bmatrix}Q_{4m_1}Q_{4m_2}Q_{6m_3}\ , \tag{3.18}$$

where F_4 and F_6 are given by Eq. (3.3). Nonzero Q_{lm}'s can be *generated* even if they do not minimize the corresponding free energy F_l. The coupling $w_{6,4}$, for example, shows that nonzero $l=6$ spherical harmonics can act like an ordering field which couples linearly to the Q_{4m}, generating $l=4$ spherical harmonics if these are not already present. In order for this not to happen, the $l=6$ spherical harmonics must satisfy nine nonlinear equations, namely

$$\sum_{m_1+m_2=-m}\sum_{m_2}\begin{bmatrix}6&6&4\\ m_1&m_2&m\end{bmatrix}Q_{6m_1}Q_{6m_2}=0\ ,$$
$$m=-4,-3,\ldots,+4\ . \tag{3.19}$$

Since there is a three-dimensional manifold of equivalent states related by rotations for any l, these nine constraints completely specify an $l=6$ state, up to a rotation and an overall amplitude. It can be checked that the icosahedral state, with $Q_{60}^2=11\,|\,Q_{6\pm5}\,|^2/7$ and all other $Q_{6m}=0$, satisfies (3.19). It is probably the only nontrivial solution. It can also be checked that icosahedral spherical harmonics do not generate $l=2$ order parameters, via a $w_{6,2}$ coupling. In order for nonzero Q_{4m}'s not to generate Q_{2m}'s we must have

$$\sum_{m_1+m_2=-m}\sum_{m_2}\begin{bmatrix}4&4&2\\ m_1&m_2&m\end{bmatrix}Q_{4m_1}Q_{4m_2}=0\ ,$$
$$m=-2,-1,\ldots,2\ . \tag{3.20}$$

A (probably unique) nontrivial solution to this set of five constraints is the cubic state (2.4), with all spherical harmonics except Q_{40} and $Q_{4\pm4}$ zero in the appropriate coordinate system.

The $w_{4,6}$ coupling in Eq. (3.18) shows that the cubic state can, in general, generate "harmonics" at $l=6$. Couplings like $w_{4,8}$, $w_{4,10}$, etc. suggest harmonics at even higher l values, as indeed seems the case for the cubic clusters tabulated in Fig. 2. An interesting case is the possible generation of $l=8$ order parameters by the icosahedral state. The relevant coupling term,

$$w_{6,8}\sum_{\substack{m_1,m_2,m_3\\ m_1+m_2+m_3=0}}\begin{bmatrix}6&6&8\\ m_1&m_2&m_3\end{bmatrix}Q_{6m_1}Q_{6m_2}Q_{8m_3}\ , \tag{3.21}$$

will lead to nonzero Q_{8m}'s provided

$$h_{8,m}\equiv w_{6,8}\sum_{m_1+m_2=-m}\sum_{m_2}\begin{bmatrix}6&6&8\\ m_1&m_2&m\end{bmatrix}Q_{6m_1}Q_{6m_2} \tag{3.22}$$

is nonzero for some m. It can be checked that all $h_{8,m}$ vanish identically in the icosahedral state, so that $l=8$ order parameters are in fact *not* generated,

in agreement with the icosahedral histograms in Fig. 2. Using the character tables of the icosahedral subgroup of SO(3), Mermin has shown that icosahedral harmonics can occur only for $l=10,12,\ldots$.[33]

One can also discuss the effect of the periodic boundary conditions imposed in most computer simulations within Landau's formalism. The cubic symmetry of these boundary conditions will clearly favor the $l=4$ state of cubic bond-orientational order. We can model its effect by adding a term,

$$\sum_{m=-4}^{4} h_{4m} Q_{4m}^{*} \quad , \tag{3.23}$$

to Eq. (3.18). In a coordinate system aligned with the periodic boundary conditions, we expect that the coefficients $h_{4,m}$ may be written in vector form as

$$h_{4,m}=(h_4,0,0,0,(\tfrac{14}{5})^{1/2}h_4,0,0,0,h_4)$$

$$\text{for } m=-4,-3,\ldots,+4 \quad . \tag{3.24}$$

The constant h_4 measures the strength of the cubic bias of the boundary conditions. This effect turns out to be very small in our 864-atom samples at high temperatures.

Periodic boundary conditions can have a much more pronounced effect at low temperatures, particularly when a state with extended orientational order starts to form. Interaction of the icosahedral order with the boundary conditions can produce an effective cubic field which is much stronger than that displayed in Eq. (3.23). Indeed, we can model this situation by an effective free energy

$$F_{\text{eff}}=F+\sum_{m=-4}^{4} h_{4m}Q_{4,-m} + w \sum_{\substack{m_1,m_2,m_3 \\ m_1+m_2+m_3=0}} \begin{pmatrix} 6 & 4 & 4 \\ m_1 & m_2 & m_3 \end{pmatrix} \times Q_{6m_1}h_{4m_2}Q_{4m_3} \quad , \tag{3.25}$$

where F is given by (3.18). The two couplings involving the field h_{4m} due to the periodic boundary conditions are designed to be invariant under a simultaneous rotation of the boundary conditions and the relevant order parameters. The coupling proportional to w becomes important when Q_{6m} is nonzero. The result is an enhanced effective cubic field

$$h_{4m}^{\text{eff}}(T)=h_{4m}+w \sum_{\substack{m_1 \\ m_1+m_2=-m}} \sum_{m_2} \begin{pmatrix} 6 & 4 & 4 \\ m_1 & m_2 & m \end{pmatrix} \times Q_{6m_1}(T)h_{4m_2} \quad . \tag{3.26}$$

By applying a strong, icosahedral ordering field to our sample at low temperatures we have in fact been able to generate the nonzero *cubic* spherical harmonics predicted by (3.26). It would be hard to understand this result in the absence of a coupling between icosahedral order and the periodic boundary conditions.

C. Orientational order versus translational order

An order parameter theory of the liquid-to-solid transition was constructed in the 1930s by Landau himself.[39] Just as in the case of the orientational free energies (3.3), the existence of a third-order invariant suggests that this transition must be first order. Baym *et al.*[40] have shown that the third-order term favors a bcc crystal structure. Since Landau's approach assumes an expansion in a small order parameter, this observation is strictly valid only in the limit of a vanishingly small first-order transition. This bias toward bcc crystals was rediscovered by Alexander and McTague,[41] who also noted that a hypothetical "icosahedral crystal" would be the most favorable structure of all. They argued that the tendency toward local icosahedral order could be understood in this way.

In our view, the most convincing argument for local icosahedral order is the energetic one originally proposed by Frank.[8] One does not need to be close to a vanishingly small first-order transition. In our numerical studies, we have found no evidence for icosahedral density waves. Although a space-filling icosahedral density wave is impossible, one might expect subsets of the allowed wave vectors to order, or abnormally persistent oscillations in the radial distribution function. The icosahedral order we do find refers to a *different* order parameter.

To clarify this distinction, consider a Landau free energy which depends on both translational and orientational order parameters. Translational order is described by the Fourier components $\rho_{\vec{G}}$ in the Fourier expansion of the mass density $\rho(\vec{r})$ (Ref. 39)

$$\rho(\vec{r})=\rho_0+\sum_{\vec{G}} \rho_{\vec{G}} e^{i\vec{G}\cdot\vec{r}} \quad , \tag{3.27}$$

where the sum is over possible reciprocal-lattice vectors $\vec{G}$. The orientational order parameters displayed in Eq. (3.2) can be combined with the $\rho_{\vec{G}}$'s to give a free energy

$$\mathcal{F}=\frac{1}{2}r_T\sum_{\vec{G}}|\rho_{\vec{G}}|^2+w_T\sum_{\substack{\vec{G}_1,\vec{G}_2,\vec{G}_3\\ \vec{G}_1+\vec{G}_2+\vec{G}_3=0}}\rho_{\vec{G}_1}\rho_{\vec{G}_2}\rho_{\vec{G}_3}+\cdots+\frac{1}{2}r_6\sum_{m=-6}^{6}|Q_{6m}|^2$$
$$+w_6\sum_{\substack{m_1,m_2,m_3\\ m_1+m_2+m_3=0}}\begin{pmatrix}6&6&6\\ m_1&m_2&m_3\end{pmatrix}Q_{6m_1}Q_{6m_2}Q_{6m_3}+\cdots+\gamma\sum_{\vec{G}}\sum_{m=-6}^{6}Y^*_{6m}(\theta_{\vec{G}},\phi_{\vec{G}})Q_{6m}|\rho_{\vec{G}}|^2\ . \tag{3.28}$$

Here, $\theta_{\vec{G}}$ and $\phi_{\vec{G}}$ are the polar angles associated with $\vec{G}$, and we have displayed only the $l=6$ orientational order parameters for simplicity. The summations over $\vec{G}$ are typically restricted to a spherical shell with a radius corresponding to the first maximum of the structure function in reciprocal space.[39] With decreasing temperatures, either the translational or the orientational degrees of freedom will order first, depending on the values of the temperature-dependent coefficients r_T and r_6. Alexander and McTague discuss the translational order embodied in an icosahedral subset of nonzero $\rho_{\vec{G}}$'s.[41] Our numerical studies, however, seem better interpreted as an ordering of the Q_{6m}'s, rather than of the $\rho_{\vec{G}}$'s.

The coupling proportional to γ in Eq. (3.28) shows that a nonzero translational order parameter acts like an ordering field on the bond order. Thus, long-range orientational order must accompany any periodic density wave. This same term, however, only couples bond order to the square of the translational order parameter. Translational order is not automatically generated by bond order. This asymmetry between translational and orientational order was emphasized in a more physical way in the first paragraph of the Introduction.

D. Structure function

The Landau expansion (3.28) implies a modulation of the structure function in the presence of bond-orientational order. The argument given for cubic bond order in Ref. 16 leads to the prediction

$$S(\vec{q})\equiv\langle|\rho_{\vec{q}}|^2\rangle=\frac{k_BT}{r_T+2\gamma\sum_m Y^*_{6m}(\theta_{\vec{q}},\phi_{\vec{q}})\langle Q_{6m}\rangle}\ . \tag{3.29}$$

If $\langle Q_{6m}\rangle$ is nonzero, and represents, say, an icosahedrally oriented state, Eq. (3.29) predicts a direction dependence in $S(\vec{q})$ with the same symmetry. The γ coupling in Eq. (3.28) shows that nonzero bond order breaks rotational invariance in reciprocal space. If a solid crystallizes at a still lower temperature, it will be aligned with the directions singled out by the bond order.

IV. ORIENTATIONAL ORDER IN A LENNARD-JONES LIQUID

A. Molecular-dynamics simulation

In this section, we describe simulation results for particles subject to the Lennard-Jones potential

$$V(r)=4\epsilon\left[\left[\frac{\sigma}{r}\right]^{12}-\left[\frac{\sigma}{r}\right]^{6}\right]\ , \tag{4.1}$$

where $r_0=2^{1/6}\sigma$ corresponds to the potential minimum, and $-\epsilon$ is the corresponding minimum energy. The atomic mass of the atoms in the models will be designated as m. The Lennard-Jones potential is often used to model simple liquids and metallic glasses. In our discussions of Lennard-Jones models, units of dimensional quantities such as energy, density, length, and temperature will be scaled in units of σ, ϵ and m so as to make them dimensionless numbers [in particular, $T^*=k_BT/\epsilon$ and $\rho^*=\rho(\sigma^3/m)$]. Time is measured by $\tau^*\equiv t(\sigma^2/m\epsilon)^{1/2}$. Such units are standard "Lennard-Jones units"; they can be converted to units appropriate for argon by using $\epsilon/k_B=120$ K, $r_0=3.4$ Å, and $m=40$ amu. Lennard-Jones models will be denoted LJ in our shorthand. Most of our runs were done with density $\rho^*=0.973$. With this choice, the pressure is nearly zero at the melting temperature $T^*_m=0.701$.[72]

Our simulations were carried out via the molecular-dynamics technique[4]: A fixed number of particle positions inside a periodic box are randomly chosen along with a set of random initial velocities. The instantaneous forces on each atom due to his neighbors are computed from the potential. From the instantaneous accelerations, new positions and velocities are computed. Our molecular-dynamics time unit is $\tau_0=4.64\times10^{-3}(\sigma^2m/\epsilon)^{1/2}=10^{-14}$ sec. These last two steps are repeated many times over until equilibrium is achieved, and the velocities scaled so that the equilibrium model corresponds to a chosen temperature. The model may then be cooled by removing a small percentage of the kinetic energy (less than 1%) each step until the desired

temperature has been (approximately) reached and then the model is relaxed at least 1000 more steps to ensure equilibrium. It is important that during cooling only a small percentage of the kinetic energy is removed in order to remain as close to equilibrium as possible. Further relaxation assures that equilibrium has been reachieved. The models are relaxed for a total of 10000 to 70000 molecular-dynamics time steps, including steps for quenching. Our run times and sample sizes (≤ 864 particles) are about at the limit of what is possible on a modern high-speed computer.

The equilibrated LJ models may be classified according to the quench procedure that is used to generate them. If the model is quenched directly from a high-temperature model we will refer to it as a "direct-quench" (DQ) model. Depending on how small a percentage of the kinetic energy that is removed each molecular-dynamics step, the quench will be referred to as fast (1%) or slow (0.1%) corresponding to 10^{13} and 10^{12} K/sec, respectively. Even the slowest quench calculable on the computer is rapid compared to any experimental quenching process ($< 10^7$ K/sec). In some cases a model has been obtained through a sequence of quenching a few degrees, relaxing 5000 steps, quenching again, etc. A model so obtained will be referred to as a sequentially quenched (SQ) model. The growth of bond order with decreasing temperature was most pronounced in the sequentially quenched samples.

B. Orientational order

A histogram of Q_l vs l for an 864-atom SQ-LJ model with $T^* = 0.719$ (equilibrated 30000 steps at that value of T^*) is shown in Fig. 4(a). The averages over the bonds in Eq. (2.1) are evaluated by summing all bonds in a sphere of radius 7 centered within the periodic cell used for the molecular-dynamics computation (the units of length are chosen such that the first peak in the radial distribution function occurs at $r = 1$). Bonds which extended outside the periodic cell were excluded. The side of the box for the 864-atom model with density $\rho^* = 0.973$ has a length of 8.56 in these units. The histograms for $T^* = 0.719$ were found to decrease steadily with increasing averaging volume. The melting temperature for the LJ solid is $T_m^* = 0.701$. Superimposed on the figure are Q_l's found by using a random-number generator to produce the same number of bonds but with an isotropic distribution of directions. The two histograms appear to be virtually indistinguishable with a possible weak signal at $l = 6$. Evidently, the orientations of nearby clusters are uncorrelated at $T^* = 0.719$. In contrast, Fig. 4(b) shows the histogram of Q_l vs l for a SQ model with $T^* = 0.554$. The signal at $l = 6$ is particularly large, and rather insensitive to the averaging volume. The result suggests extended correlations in the orientations of bonds, possibly with an icosahedral symmetry. Although the signal at $l = 4$ is rather weak, a glance at the histograms in Fig. 2 shows that a more sophisticated test is necessary to rule out cubic orientational order. Also, the size of the $l = 8$ signal (which would be zero for a perfect icosahedron), suggests that some cubic order may be present.

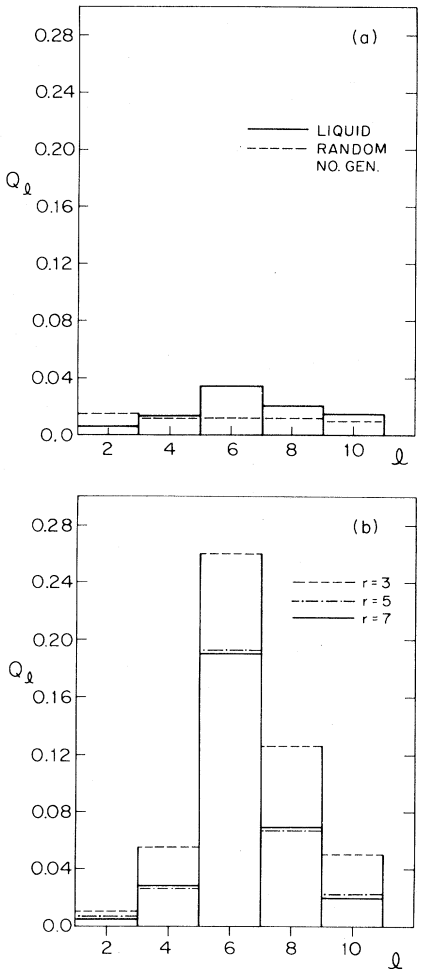

FIG. 4. (a) Quadratic invariants Q_l for a high-temperature Lennard-Jones liquid (solid lines). The dashed lines indicate averages obtained using a random-number generator to produce the orientations of an equivalent number of bonds. (b) Q_l histograms for a supercooled Lennard-Jones liquid. The dependence on the radius (r) of the averaging volume is shown: a dashed line, $r=3$; dotted-dashed line, $r=5$, solid line, $r=7$.

One's first concern is that the appearance of orientational order in a model supercooled below the

melting temperature might be an indication of the onset of crystallization. A sensitive test of crystallization is to study the temperature and pressure of the model as a function of relaxation time. Figures 5(a) and 5(b) show this dependence in a series of samples including at $T^*=0.719$ and $T^*=0.554$. Although there are fluctuations, the temperature and pressure are more or less constant over the entire relaxation interval for the samples shown in Fig. 4. The histograms in Fig. 4 were taken from a sample generated near the middle of the time range shown in Figs. 5(a) and 5(b). By contrast, consider the sharp change in the temperature and pressure curves in Figs. 5(a) and 5(b) found for a supercooled sample at $T^*\cong 0.4$ that apparently has undergone crystallization. In a plot of the projection of the atoms taken at a time well after the sharp change an fcc crystalline configuration can be discerned by eye. Further tests of crystallization can be found in examining the radial distribution function. In Figs. 6(a) and 6(b) are shown the radial distribution functions for the samples at $T^*=0.719$ and $T^*=0.554$, which are what are expected for a (supercooled) liquid above the glass transition.[23] In Fig. 6(c) is shown the sample which the first test indicated had

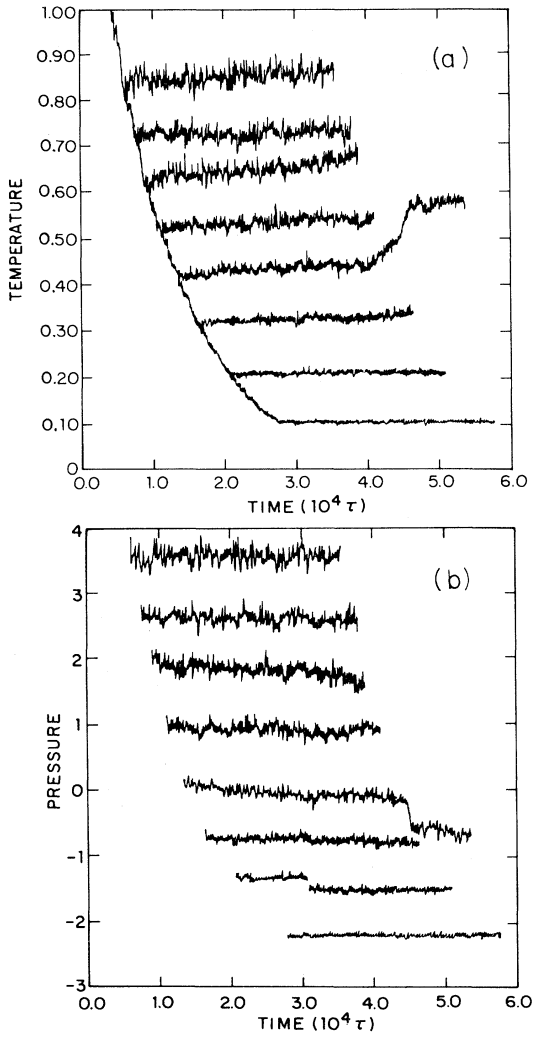

FIG. 5. Time dependence of the (a) temperature and (b) pressure (arbitrary units) for a sequence of molecular-dynamics runs. The abrupt changes in the fifth curve from the top at $10^4\tau\approx 4.6$ indicates the onset of crystallization. The break in the seventh pressure curve from the top suggests that crystallization may have occurred in this run as well. (The order of samples is the same from top to bottom in the two figures.)

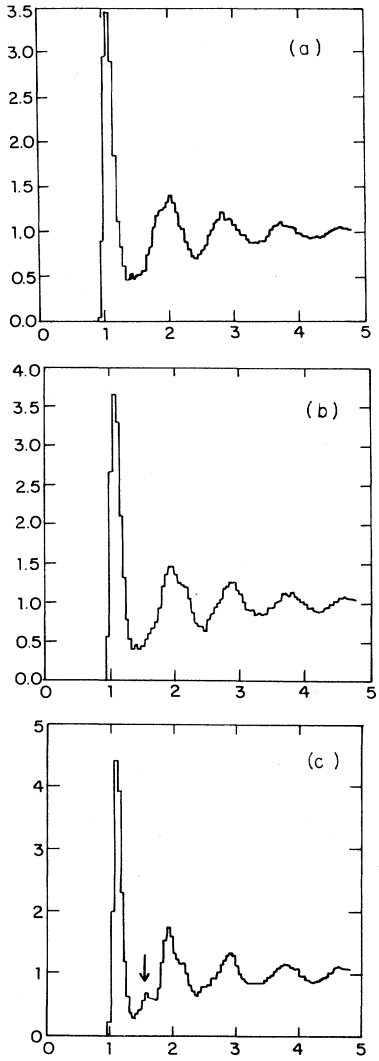

FIG. 6. (a) and (b) show the radial distribution functions (RDF) for the high- ($T^*=0.719$) and low- ($T^*=0.554$) temperature samples whose orientational order is displayed in Fig. 4. (c) shows the RDF for a sample which has crystallized. The extra peak is indicated by the arrow.

undergone crystallization (measured a short time after the drop in temperature and pressure). The critical difference is that there appears an additional small peak for the crystallized sample between the first- and second-nearest-neighbor peaks of the uncrystallized samples. The temperature, pressure, and radial distribution function tests have been found in all our computer experiments to yield consistent checks for crystallization and all samples we present as bond-oriented models pass these tests as *uncrystallized samples.*

More information about the bond-orientational order can be obtained from the bond-angle correlation functions:

$$G_l(r)=\frac{4\pi}{2l+1}\sum_{m=-l}^{l}\langle Q_{lm}(\vec{r})Q_{lm}(\vec{0})\rangle/G_0(\vec{r}) \ , \tag{4.2a}$$

where

$$G_0(\vec{r})=4\pi\langle Q_{00}(\vec{r})Q_{00}(\vec{0})\rangle \ , \tag{4.2b}$$

and the angular brackets indicate an average over all atoms separated by $\vec{r}$. The values of Q_{lm} were computed according to the orientation of that bond with respect to a fixed external coordinate system. The angular brackets in Eqs. (4.2) then indicate an average over all bonds separated by $\vec{r}$, where the "position" of a bond was defined as the coordinates of the middle of that bond. The correlations are divided by $G_0(\vec{r})$, which is just the bond-density—bond-density correlation function, to approximately account for effects due to the positional disorder in the locations of the bonds. The definition of $G_l(\vec{r})$ insures that it is fixed at unity for all r if all bonds correspond to exactly the same spherical harmonics. Since $G_0(\vec{r})$ tends to a constant for large r, the *limiting* behavior of $G_4(\vec{r})$ and $G_6(\vec{r})$ is unaffected by this division.

The correlation functions were measured by associating each bond in the periodic box with the vertices of a cubic $N\times N$ mesh (typically $N=8$ or 16 was found to give satisfactory results for the 864-atom model). The Q_{lm} were computed with respect to a fixed coordinate system and assigned to the eight vertices with a weighting depending on the bond's proximity to a given vertex. Partitioning all bonds in this way led to a set of Q_{lm} associated with each mesh intersection point. Correlations for $l=0$, 4, and 6 could then be computed straightforwardly and efficiently by fast Fourier transform techniques. The results for a $T^*=0.554$ sample is shown in Fig. 7 with the results for a $T^*=0.710$ sample shown in the inset. Both samples were prepared as in Fig. 4. Correlations for both $l=4$ and $l=6$ fall off rapidly in the high-temperature sample. The decays appear to be exponential with approximately the same

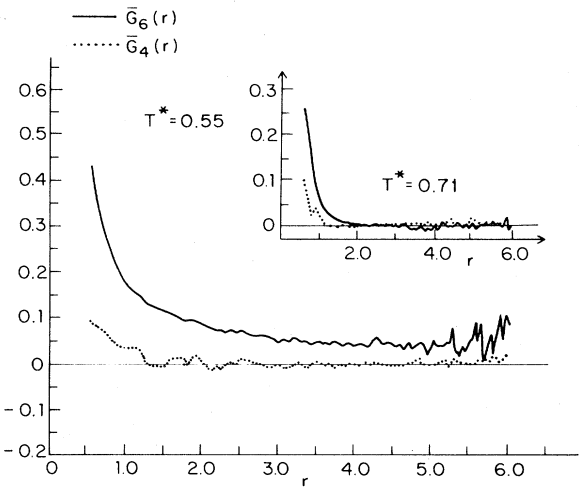

FIG. 7. Orientation correlation functions in high- and low-temperature samples.

correlation length, as one would expect for an isotropic liquid. In contrast, $G_6(\vec{r})$ appears to approach a nonzero constant for large r at $T^*=0.554$. There are however, no persistent correlations in $G_4(\vec{r})$, suggesting the absence of crystallization or the cubic bond-orientational order proposed by Nelson and Toner.[16] When samples did begin to crystallize we observed immediate significant changes in $G_4(\vec{r})$. The correlation function is a useful test of the presence of bond-orientational order and of its range. Behavior very similar to that found for $G_6(\vec{r})$ for the sample with $T^*=0.554$ has been found for a hexatic orientational correlation function in *two*-dimensional "Lennard-Jonesium" by Frenkel and McTague.[43]

Many samples were analyzed to determine the orientational symmetry breaking as a function of temperature. Figure 8 shows the order parameter $Q_6(T^*)$ which can be extracted from the asymptote of $G_6(r)$, via

$$\lim_{r\to\infty} G_6(\vec{r})\equiv\bar{Q}_6^2 \ . \tag{4.3}$$

Evidently, $\bar{Q}_6(T^*)$ becomes nonzero below $T^*=0.626$. Above this temperature, we show an orientational correlation length $\xi_6(T^*)$ determined by exponential fits to $G_6(\vec{r})$. Each sample was obtained in sequence by quenching the preceding sample (beginning with $T^*=1.29$) and equilibrating $10\,000\tau_0$. Figure 8 suggests a transition to an icosahedral phase at $T_c^*=0.63$ indicated by an increase in the orientational correlation length. The radial distribution function does not change significantly through this transition. No anomaly in the specific heat could be observed as the temperature dropped below T_c^*, but there are large uncertainties

in T^* and in the energy density difference that makes it difficult to make precise measurements of the specific heat in computer simulations. Our results are consistent with either a continuous or a weakly first-order transition.

As discussed in Sec. II, the quantity $\hat{W}_6$ [see Eq. (2.2)] provides a sensitive way of distinguishing between icosahedral and cubic order. Well below the apparent ordering temperature in Fig. 8, at $T^*=0.554$ we found

$$\hat{W}_6(T^*=0.554)=-0.060\,939 \ . \tag{4.4}$$

Although $|\hat{W}_6(T^*=0.554)|$ is about 4.6 times greater than the value (3.12) characterizing cubic orientational order, it is only 35% of the value (3.9) for perfect icosahedral order. In an infinite system, we would expect that

$$|\hat{W}_6(T)| = |\hat{W}_6^{\text{icos}}| = 11/\sqrt{4199} \tag{4.5}$$

at all temperatures below a transition to extended icosahedral order. This deviation from perfect "icosahedrality" is due at least in part to the effect of cubic periodic boundary conditions on our small samples. A degree of cubic order is suggested by the small signal at $l=4$ in Fig. 4(b), and the somewhat larger one at $l=8$. As discussed in Sec. III B, periodic boundary conditions promote cubic order, in a way which is enhanced by the presence of extended icosahedral order [see Eq. (3.25)]. A superposition of several different icosahedral "domains" would also lead to a reduced value of $|\hat{W}_6|$. By "domains" we mean, for example, situations where the icosahedral order parameter has been twisted up like a Moebius strip due to the periodic boundary conditions.

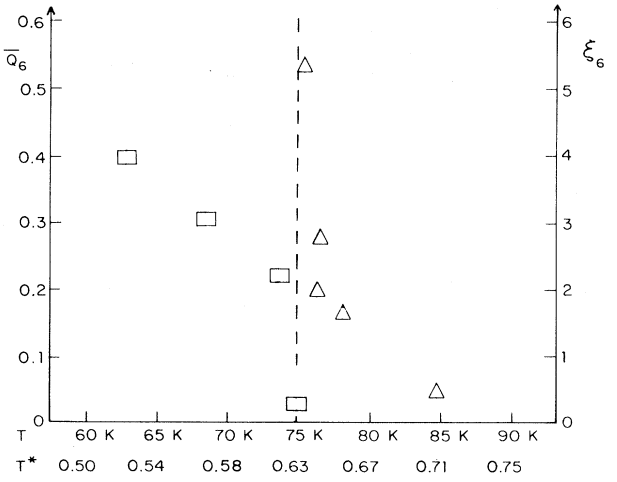

FIG. 8. Orientational correlation length ξ_6 (triangles) and "order parameter" Q_6 (squares) as a function of temperature. The temperature is given both in reduced units and in units appropriate to liquid argon.

To study these questions further, we have searched for a preferred coordinate system using Eq. (2.6). As discussed in Sec. II, it should be possible in icosahedral samples to find a set of reference axes such that only Q_{60} and $Q_{6\pm5}$ are nonzero. Furthermore, these quantities must obey the relation (2.5). A search was made for the set of Euler angles which minimized the Q_{6m}'s with m not equal to 0 and ±5 in a variety of bond-oriented samples. Then the ratio $|Q_{60}|/|Q_{65}|$ was computed. For several samples the ratio agreed to within 10% of the magic ratio indicating a high degree of icosahedral correlation. Other samples were better described as a superposition of icosahedral domains, or a superposition of cubic and icosahedral order. To test the domain idea we performed the test on two perfect icosahedra rotated with respect to one another and we found that unless the angles were aligned to within 5% (about a given axis) the special ratio (2.5) was not obtained. Thus, the samples that passed, this "rotation test" demonstrated a high degree of icosahedral correlation over the full volume of the sample.

The test also serves as a method of distinguishing icosahedral order from dodecahedral order. The test not only yields the ratio of the absolute values of Q_{60} and Q_{65}, but also their relative sign, in a coordinate system such that Q_{65} is real and positive. In all samples that passed the test the relative sign was found to be negative, corresponding to icosahedral rather than dodecahedral order.

Curiously enough, different molecular-dynamics samples required nearly equivalent sets of Euler angles in order to minimize the Q_{6m}'s with $m\neq0,+5,-5$. Furthermore, the Euler angles that were found by the random search corresponded to a rotation about one of the original coordinate axes (aligned with the periodic box) by an angle $\tan\theta=1/\tau$ where τ is the "golden ratio," $\tau=(\sqrt{5}+1)/2$. To understand this result, recall that the 12 atoms on the surface of an icosahedron actually lie in three mutually perpendicular rectangles (see Fig. 9). If one tries to place a sample with extended order of this kind in a box (such as the periodic box used in the molecular-dynamics runs) the icosahedron will evidently try to orient itself such that each rectangle is parallel to a side of that box. Each rectangle has sides with lengths in the golden ratio. As a result, the fivefold symmetry axis of the icosahedron, which corresponds to one of the diagonals of the rectangles, is rotated by an angle

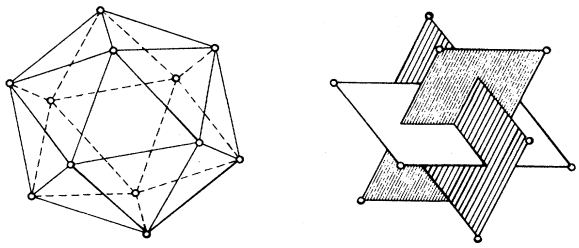

FIG. 9. View of the 12 atoms making up the surfaces of an icosahedron, together with their decomposition into three orthogonal rectangular planes.

$\tan\theta = 1/\tau$ from the z axis of the box. It appears that the periodic boundary conditions weakly influence the developing icosahedral bond-orientational order in much the same way as a weak magnetic field can influence the magnetization in a ferromagnet near the Curie temperature. The periodic box cannot cause the icosahedral ordering, however; long-range correlations are required to transmit the information about the icosahedral orientation from a surface to the center of the box. Any orientational order induced directly by the periodicity must, of course, be cubic.

As discussed above, this coupling to the periodic boundary conditions limits the perfection of an emerging icosahedral state. An analogous suppression of noncrystallographic "amorphon" clusters by periodic boundary conditions has been emphasized by Hoare.[11] From this point of view, the amount of icosahedral order we do observe in our supercooled samples is remarkable.

C. Icosahedral ordering field

To eliminate domain effects and to counteract in an interesting way the periodic boundary conditions, we repeated our simulations of 864 particles using a Lennard-Jones potential augmented by an icosahedral direction-dependent part. Although direction-dependent, this pair potential is translationally invariant,

$$V(\vec{r}) = 4\epsilon\left[\left[\frac{\sigma}{r}\right]^{12} - \left[\frac{\sigma}{r}\right]^{6}\right] - \left[\sum_{m=-6}^{6} h_{6,m} Y^{*}_{6,m}(\theta_r,\phi_r)\right] f(r) \,. \quad (4.6)$$

Here, (θ_r,ϕ_r) are the polar angles of the line joining two particles measured with respect to an external coordinate system. In the special coordinate system discussed at the end of Sec. IV B [i.e., one obtained by rotating by $\theta = \tan^{-1}(1/\tau)$ about one of the coordinate axes of the periodic box], we have

$$h_{6,m} = h_6(0, -(\tfrac{7}{11})^{1/2}, 0,0,0,0,1,0,0,0,0, (\tfrac{7}{11})^{1/2}, 0), \quad m = -6, -5, \ldots, 0, \ldots, +6 \,. \quad (4.7)$$

The function $f(r)$ smoothly cuts off the icosahedrally symmetric angular part of the interaction beyond $r = 1.2$. Cooling with $h_6 = 0.05$ produced a nonzero icosahedral order parameter at all temperatures, as one might expect. The response was quite weak above T_c^*, however, and much larger values of Q_6 were produced below this temperature. After quenching to a temperature, $T^* = 0.523$, the sample was equilibrated 3000 steps under the influence of the modified LJ potential and then another 3000 steps under the influence of the ordinary LJ potential. During this process the temperature rose to $T^* = 0.536$. (Had h_6 been turned off sufficiently slowly, one might have expected the temperature to decrease, in analogy to adiabatic cooling of spins in a magnetic field.) The state achieved in this way (via a fast quench) had quite extended correlations (see Fig. 10) in $G(r)$ yielding an estimate of Q_6 more than twice as large as obtained without the direction-dependent potential. The nonzero Q_{6m} that remained reflected the icosahedral symmetry of the perturbation as found by rotating the Q_{6m}'s so as to find the special ratio or by computing the W_l's. These results are consistent with a picture of icosahedral domains aligned by first cooling with h_6, and then remaining aligned after turning off this perturbation. The sample at $T^* = 0.536$ was eventually quenched to $T^* = 0.05$, where it remained icosahedrally oriented (without a substantial increase in Q_6) and noncrystalline for some 30 000 time steps.

For stronger icosahedrally orienting perturbations, we found weaker but extended correlations in $G_4(\vec{r})$ as well, although the radial distribution function indicated an absence of crystallization. This peculiar effect results from the interaction of the icosahedral order parameter and periodic boundary conditions discussed in Sec. III B. Figure 11 shows the correlation function and radial distribution function for the sample that was relaxed under the strong potential. The coupling h_6 was reduced in five equal increments each followed by 1000 time steps of equilibration (all done at a roughly fixed temperature). The results are shown in Fig. 11(a).

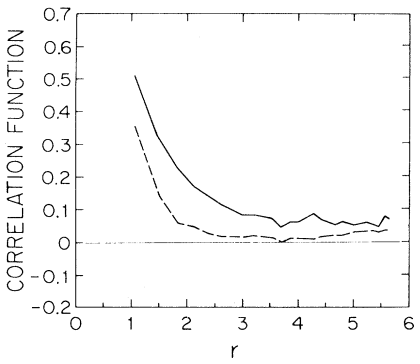

FIG. 10. The orientational correlation function $G_6(r)$ obtained by cooling in a small icosahedral field, turning this field off, and then equilibrating (solid line). For comparison, we show $G_6(r)$ for a sample cooled at the same rate without an icosahedral field (dashed line). Both samples were cooled more rapidly than in the low-temperature sample shown in Fig. 7.

Note the extended correlations in $G_4(\vec{r})$. The sample was then relaxed a further 4000 time steps and the results are shown in Fig. 11(b). Note that $G_4(\vec{r})$ has been reduced. Compared to the correlation functions in other samples, the icosahedral correlation in these samples appears to be enormous. The radial distribution function [Fig. 11(c)] appears to be somewhat distorted compared to a sample cooled in the absence of the icosahedral perturbation.

D. Dependence on quench rate, density, and sample sizes

The degree of bond-orientational correlation is sensitive to the quench rate used to cool the sample from the high-temperature state. The samples discussed above were quenched at the "slow" rate of 10^{12} K/sec. We found that the slower the quench rate, the greater the icosahedral correlation for a given number of molecular-dynamics steps. In particular, for a sample sequentially quenched to $T^*=0.508$ from a temperature of $T^*=1.29$ with a "fast" quench rate of 10^{13} K/sec, no measurable orientational correlations were found after 30 000 molecular-dynamics steps. The sample was reheated to a temperature of $T^*=0.667$ (above the apparent critical temperature for the transition to the oriented phase), and slow-quenched again at the old rate to $T^*=0.525$. The sample then showed typical icosahedral bond-orientational correlations (see Fig. 8) for that temperature. Of course, experimental samples are quenched at rates much *slower* than we can simulate. The fact that we reproduce our original results with a sample that has been "fast-

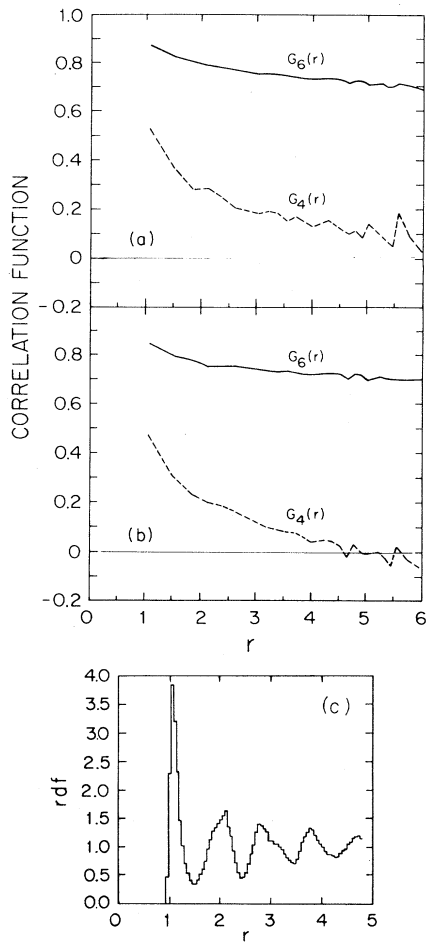

FIG. 11. (a) Correlations $G_6(r)$ (solid) and $G_4(r)$ (dashed) obtained after cooling in a strong icosahedral field. The nonzero asymptotic for $G_4(r)$ is due to the interaction between icosahedral order and the periodic boundary conditions. (b) $G_6(r)$ (solid) and $G_4(r)$ (dashed) for the same sample after the strong field was totally removed and the sample further equilibrated. (c) RDF for the sample in (b).

quenched", reheated somewhat, and then "slow-quenched" is encouraging.

Samples have also been run in which the initial density was changed from 0.973 to 1.053. In Fig. 12 is shown the phase diagram for LJ liquids and one observes that this change in density represents a significant shift in the melting temperature from $T^*=0.701$ to 1.30. A SQ series of samples containing 864 atoms was produced beginning from $T^*=1.51$ to $T^*=0.753$. Beginning at a critical temperature of $T^*=1.15$, the bond-orientational correlation function was found to approach a nonzero value asymptotically. The behavior of the higher-density samples was virtually identical to the origi-

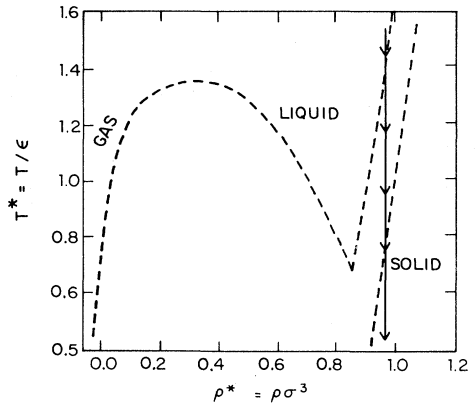

FIG. 12. Phase diagram for a Lennard-Jones liquid (adapted from Ref. 42). The arrow shows the thermodynamic path taken on most of the runs discussed in this paper ($\rho^*=0.973$). Qualitatively similar results were obtained upon supercooling at a higher density, $\rho^*=1.053$.

nal samples and the ratio of the critical temperature to the melting temperature was found to be approximately 0.9 in both cases.

We have performed many tests with samples of different sizes. An extensive study of runs carried out on 600 particles, while maintaining the density $\rho^*=0.973$ gave results qualitatively similar to those reported for the 864-atom models. We have also performed some experiments with a larger 1200-atom model. The 1200-atom model was too large to perform detailed tests of the behavior of the correlation function as a function of temperature, but samples were generated below the critical temperature (0.626) for the 864-atom model that exhibited long-range bond-orientational order according to the orientational correlation functions.

V. ORIENTATIONAL ORDER IN MODELS OF METALLIC GLASSES

A. Finney model

Dense-random-packing models, inspired by the original work of Bernal,[25] are often used to model structure in metallic glasses. The Finney model, in particular, was created by pouring 8000 hard spheres into a bladder with a roughened interior and filled with hot wax. The bladder was kneaded to simulate annealing, the wax allowed to cool, and the particle coordinates measured.[24] These initial conditions were then relaxed in a Lennard-Jones potential by a conjugate-gradient computer program which seeks a local minimum in the potential energy. The radial distribution functions obtained from the relaxed Finney model agree well with x-ray diffraction data from metallic glasses.[14]

Figure 13 shows the quadratic invariants Q_l obtained by averaging over spherical pieces of the relaxed Finney containing 853, 1753, and 3701 particles. Although still visible for 3701 particles, the bond-orientational order decreases steadily with averaging volume. For the 3701-particle sample we found $\hat{W}_6=0.038\,429$; about 3 times larger than the cubic value (3.12), but only 22% of the value (3.9) for a state with perfect icosahedral order. It seems likely that orientational order in the relaxed Finney model vanishes in the limit $N\to\infty$, suggesting the view that this particular dense-random-packing model is macroscopically much like an isotropic liquid. Also shown in Figure 13 are the Q_l's obtained from our most orientationally ordered (but noncrystalline) molecular-dynamics simulation of 864 particles ($T^*=0.55$). These signals are more than twice as large as those in the 853-atom Finney model. It is possible, of course, that the Q_l obtained from molecular-dynamics simulations also became systematically smaller in the limit of very large sample sizes.

Hoare[11] has suggested that the hard-sphere initial conditions of most dense-random-packing models represent artificially "jammed" configurations which are inaccessible to particles cooled under laboratory conditions in a soft potential. From this point of view, it is interesting that our "best" molecular-dynamics sample has more than twice the orientational order in the corresponding Finney model. One might expect even more orientational order in liquids supercooled at the very slow rates available in the laboratory.

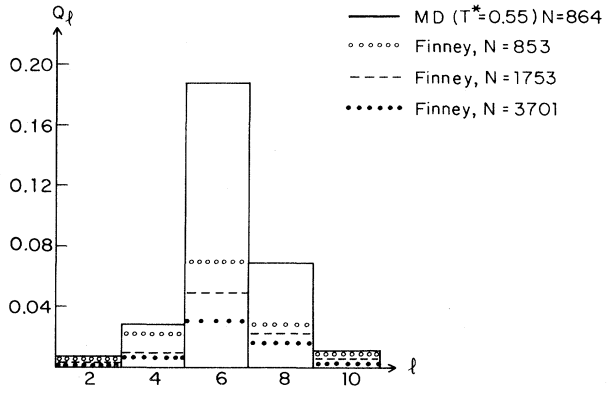

FIG. 13. Orientational order in the relaxed Finney model as a function of averaging size. The solid lines show histograms for a well-ordered molecular-dynamics sample with approximately the same number of particles as in the 853-particle Finney model.

B. Amorphon clusters

Alternatives to hard-sphere dense-random-packing models have been reviewed by Hoare.[11] Upon relaxing various clusters designed with a high degree of (noncrystalline) symmetry, one can obtain particle aggregates with anomalously low energies. Although different from hard-sphere dense-random-packing models, large clusters of this kind also give reasonable agreement with the radial distribution functions observed in metallic glasses.[11]

Figure 14 shows histograms of Q_l and W_l obtained by summing over bonds in three of the clusters discussed by Hoare. The clusters are a 13-atom icosahedron, a 43-atom "icosadodecahedron," and a 127-atom "rhombicosidodecahedron." Starting with particle coordinates with the appropriate symmetry, these structures were relaxed using a conjugate-gradient computer program. The degree of icosahedral orientational order which results is quite striking, especially when compared with the Finney model. Surface bonds were included in the averages; it is interesting to contrast the result for the simple icosahedron with those displayed in Fig. 2(a), where surface bonds were excluded. The magnitudes of the Q_l and W_l (and the sign of the W_l) oscillate with cluster size.

We find it remarkable that the 1212 near-neighbor bonds in the rhombicosidodecahedron, for example, add so coherently. Prior to relaxation, the large clusters exhibited rather poor signals, despite their overall icosahedral rotational symmetry. After relaxation, the only significant spherical harmonics which survive the averaging procedure occur at $l=6$ and $l=10$, as required for perfect bond-orientational order (see Sec. III). The values for Q_2, Q_4, and Q_8 were of order 10^{-20} in the 43-atom cluster and of order 10^{-10} in the 127-atom cluster. The values of the symmetry parameters were

$$\hat{W}_6 = -0.169\,752\ , \qquad \hat{W}_{10} = 0.093\,967\ , \tag{5.1}$$

for the 43-atom cluster, and

$$\hat{W}_6 = 0.169\,686\ , \qquad \hat{W}_{10} = 0.093\,925\ , \tag{5.2}$$

for the 127-atom cluster. The magnitudes of $\hat{W}_6$ and $\hat{W}_{10}$ are almost identical to the icosahedral values quoted in Table I. The magnitude of $\hat{W}_6$, in particular, differs by at most 0.04% from the number,

$$|\hat{W}_6^{\text{icos}}| = 11/\sqrt{4199}$$

predicted by Landau theory [see Eq. (3.9)].

Measuring bond-orientational order evidently allows one to quantify an important difference between dense-random-packing models and large amorphon clusters. The results for the 127-atom rhombicosidodecahedron, in particular, show that icosahedral bond order can propagate. As discussed in Ref. 11, this cluster can be viewed as an "icosahedron of icosahedra," with each 13-atom subunit bonded to its neighbors by octahedral bridges. Evidently, the octahedral "connective tissue" does not impair the ability of icosahedral order to add coherently across the entire structure. Measurements of bond order in even larger clusters, including those obtained via computer simulations of glassy condensation[12] would be quite interesting.

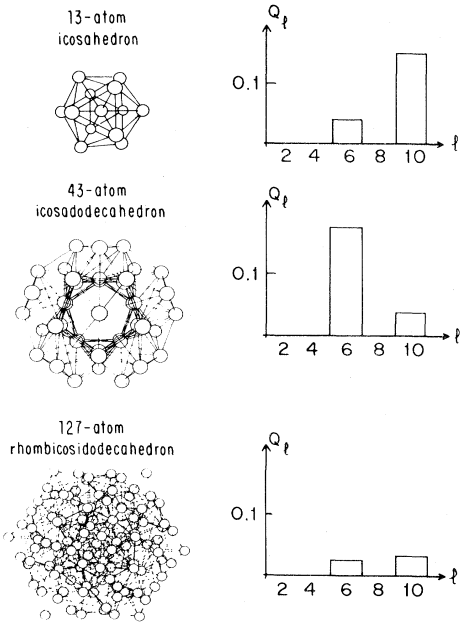

FIG. 14. Orientational histograms for several of the amorphon clusters discussed in Ref. 11.

C. Twisted orientational order

One more variant on orientational order seems worth mentioning. As pointed out by Bernal,[25] tetrahedra can be packed periodically in one dimension to form a twisted helix with three strands. (See Fig. 15). He finds these helixes throughout his dense-random-packing models. A straight average over the bonds in a spiral chain consisted of 72 tetrahedra gave numerically small Q_l's for all l, with the most prominent signals at $l=2$, 6, and 10. A much larger signal could presumably be obtained by averaging

$$Q_{lm}(\vec{r}) \equiv \sum_{m'} D^{(l)}_{m,m'}(\alpha(\vec{r}),\beta(\vec{r}),\gamma(\vec{r}))Q_{lm'}(\vec{r})\ , \tag{5.3}$$

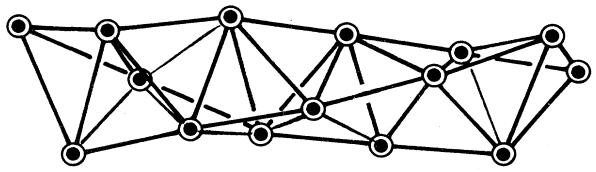

FIG. 15. Spiral packing of tetrahedra discussed by Bernal (Ref. 25).

where the Euler angles $\alpha(\vec{r})$, $\beta(\vec{r})$, and $\gamma(\vec{r})$ are chosen to untwist the spiral.

It is possible to imagine bulk analogs of this one-dimensional spiral state. With the icosahedral order parameter at each point, we associate a set of orthogonal planes via the construction illustrated in Fig. 9. States such that the orientations of these planes twist slowly in space are possible. The Bernal spiral repeats itself after about ten near-neighbor spacings, suggesting a pitch which is at least comparable to the size of our molecular-dynamics simulations.

VI. CONCLUSIONS AND SPECULATIONS ON THE GLASS TRANSITION

It is always difficult to draw firm conclusions based on small samples like those studied here. At a minimum, we hope to have demonstrated that the bond order parameters provide a useful way of quantifying and testing ideas about orientational order in liquids. It also seems clear that there is an orientational correlation length $\xi_6(T)$ which begins to exceed the range ξ_T of translational correlations in supercooled Lennard-Jones liquids at about 10% below the equilibrium melting temperature (see Fig. 8). The symmetry of the orientationally ordered state which develops has a large icosahedral component. The increase of the $l=4$ and 8 parts of the Q_l histograms at low temperatures suggests that some cubic orientational order is present as well. Our data is consistent with attributing this cubic order to the interaction of an icosahedral order parameter with the cubic periodic boundary conditions. The coupling between icosahedral order and periodic boundary conditions predicted by Eqs. (3.25) and (3.26) was confirmed by introducing an icosahedral term into the pair potential. We cannot, however, completely rule out an *intrinsic* state with mixed icosahedral and/or cubic order. Such a state would occur if both r_4 and r_6 in the free energy (3.18) become large and negative.

The bond order in the relaxed Finney model was weaker than that observed in our "best" orientationally ordered molecular-dynamics runs. This observation lends support to the suggestion by Hoare[11] that the hard-sphere initial conditions of the Finney model are unnaturally jammed, and inaccessible to real liquids upon supercooling. It should be emphasized, however, that the relative proportions of the Q_l's in the Finney model are rather similar to those observed in our computer simulations. One cannot, of course, appeal to periodic boundary conditions to account for the "cubic" signals at $l=4$ and 8 in this case.

In contrast to the Finney model, the orientational order observed in the amorphon clusters discussed by Hoare[11] is really quite striking. The symmetry is almost *perfectly* icosahedral, suggesting that this sort of bond order can propagate without difficulty across a 127-atom cluster, for example. The icosahedral order seemed unaffected by the octahedral "bridge units" used to connect neighboring 13-atom icosahedra. If confirmed by experiments on larger clusters, this would be an important observation. An analogous result holds for disordered planar ball-bearing arrays.[6] Here, information about the orientation of hard-sphere hexagons can propagate for large distances, relatively unimpeded by the disorder.

There may, in fact, be an intrinsic limit on the size of the icosahedral orientational correlation length ξ_6, due to "frustration effects." In three dimensions, one maximizes the local density by forming tetrahedral packing units. Forming icosahedra (composed of 20 such units) is an imperfect solution to the problem of packing these tetrahedra, since the bonds at the surface of a 13-atom cluster are about 5% longer than the bonds connecting surface atoms to the center. In some sense, this mismatch is what ultimately prevents a space-filling (hard-sphere) icosahedral solid, with an infinite translation-correlation length ξ_T. It is possible that long-range icosahedral orientational order is prohibited as well. Presumably, the maximum allowed ξ_6 is comparable to or larger than the size of the samples studied here.

Kleman and Sadoc[44] have proposed a description of the glassy state which starts in curved space, where a perfect icosahedral solid is possible. They then map this crystal into ordinary flat space by introducing a minimal number of disclination-line defects. Since the observed translational correlation length in real glasses is quite short, one might more profitably start with a state with perfect icosahedral *orientational* order, but very little translational order. The low-temperature description of such a state is very similar to that developed for cubic order in Ref. 16. (The hydrodynamics of icosahedral fluids is also similar to that sketched for cubic fluids in this reference.) With the local icosahedral order parameter one associates an orthonormal triad

$(\vec{l},\vec{m},\vec{n})$ corresponding to some preferred coordinate system. Low-energy excitations from the ground state are described by a slowly varying vector of rotation angles $\vec{\theta}(\vec{r})$ about these three reference directions. The corresponding long-wavelength free energy is

$$F_I=\frac{1}{2}\int d^3r\{K_a\,|\,\vec{\nabla}\times\vec{\theta}(\vec{r})\,|^2 + K_b[\vec{\nabla}\cdot\vec{\theta}(\vec{r})]^2\}\ , \tag{6.1}$$

where K_a and K_b are analogous to Frank constants in a nematic liquid crystal.[1] One now introduces the topologically stable disclination-line defects associated with (6.1). In the language of homotopy theory,[45] their law of addition is given by the homotopy group

$$\pi_1[\mathrm{SO}(3)/Y]\ , \tag{6.2}$$

where Y is the icosahedral subgroup of SO(3). These disclinations would have a lower energy than disclinations in an icosahedral solid. Also, they need not be accompanied by the grain boundaries which presumably occur in an icosahedral solid with disclinations.

We conclude with a scenario suggesting how icosahedral bond order might be related to the glass transition. Even if long-range icosahedral order is possible in liquids, it seems unlikely that

$$Q_6(T)\equiv\left[\frac{4\pi}{13}\sum_{m=-6}^{6}|\,Q_{6m}\,|^2\right]^{1/2} \tag{6.3}$$

can even approach the value it would have in a "perfect, icosahedral solid," say $Q_6=1$. Because of frustration effects in flat space, there may be a maximum value,

$$Q_{\max}<1\ , \tag{6.4}$$

bounding $Q_6(T)$ from above. One can simulate frustration in a lattice model of interacting icosahedra via the Hamiltonian

$$\mathcal{H}=-J\sum_{\langle i,j\rangle}\sum_{m=-6}^{6}Q_{6m}(\vec{r}_i)Q^*_{6m}(\vec{r}_j) + \sum_{i\neq j}\sum_{j}K(\vec{r}_{ij})_m Q_{6m}(\vec{r}_i)Q^*_{6m}(\vec{r}_j)\ . \tag{6.5}$$

Here $\vec{r}_i$ denotes a site on regular lattice, and the sum in the first term of (6.5) denotes a sum over nearest-neighbor pairs of sites. The positive interaction energy J in the first term tends to align neighbor icosahedra, described by the $Q_{6m}(\vec{r}_i)$.[22] Frustration is modeled by the much weaker longer-range interaction $K(\vec{r}_{ij})$ in the second term, which we take to vary randomly in sign, in analogy with spin glasses.[46] The coupling J favors a transition to an orientationally ordered state, which could occur well above any glass transition. The random long-range part, however, acts like a temperature-dependent random field of strength

$$h^{\mathrm{eff}}_{6,m}(\vec{r}_i)=\sum_{j\neq i}K(\vec{r}_{ij})\langle Q^*_{6m}(\vec{r}_j)\rangle\ . \tag{6.6}$$

This field becomes stronger as $Q_6(T)$ increases. Such a "feedback" of extended orientational order into a random field may prevent long-range order entirely, and will certainly limit the maximum possible orientational parameter. One might expect lengthy relaxation times just prior to the order parameter reaching its maximum possible value $Q^*_{\max}$ at an intrinsic glass transition temperature T.

ACKNOWLEDGMENTS

It is a pleasure to acknowledge discussions with P. Chaudhari, D. Turnbull, and F. Spaepen. We are indebted to N. D. Mermin pointing out that $l=8$ spherical harmonics are impossible in systems with perfect icosahedral orientational order. We also wish to thank D. Levine for aiding in the determination of the coordinates of the Hoare amorphon structures. One of us (D.R.N.) would like to acknowledge support from the National Science Foundation, through the Harvard University Materials Research Laboratory and through grant No. DMR-82-07431, as well as a grant from the A. P. Sloan Foundation. D.R.N. would also like to acknowledge the hospitality of E. Pytte at the IBM Thomas J. Watson Research Laboratories, where part of this work was carried out. One of us (P.J.S.) would like to acknowledge partial support from U.S. Department of Energy contract EY-76-C-02-3071 and a DOE Outstanding Junior Investigator Grant, as well as the continued encouragement and generous support of the IBM Watson Research Laboratories.

*Permanent address: David Rittenhouse Laboratory, University of Pennsylvania, Philadelphia, Pennsylvania 19104-3859.

†Permanent address: Dipartimento di Fisica, Libera Università degli Studi di Trento, I-381000 Trento, Italy.

[1]P. G. de Gennes, *The Physics of Liquid Crystals* (Oxford University Press, London, 1974).

[2]B. I. Halperin and D. R. Nelson, Phys. Rev. Lett. 41, 121 (1978); 41, 519(E) (1978).

[3]D. R. Nelson and B. I. Halperin, Phys. Rev. B 19, 2456

(1979).
[4]J. M. Kosterlitz and D. J. Thouless, J. Phys. C 6, 1181 (1973).
[5]For a review, see W. F. Brinkman, D. S. Fisher, and D. E. Moncton, Science 217, 693 (1982).
[6]D. R. Nelson, M. Rubinstein, and F. Spaepen, Philos. Mag. A 46, 105 (1982); D. R. Nelson, Phys. Rev. B 27, 2902 (1983).
[7]P. Chaudhari and D. Turnbull, Science 199, 11 (1978).
[8]F. C. Frank, Proc. R. Soc. London Ser. A 215, 43 (1952).
[9]Frank found that the energy of 13-atom icosahedral clusters is 8% lower than in clusters with an hcp or fcc symmetry. The magnitude of this energy difference is 3.58ϵ, where ϵ is the Lennard-Jones energy parameter. Similar preferences for local icosahedral orientational order have been found for repulsive $1/r^n$ potentials by Haymet (see Ref. 25).
[10]See, e.g., D. Turnbull, J. Chem. Phys. 20, 411 (1952).
[11]M. R. Hoare, Ann. N.Y. Acad. Sci. 279, 186 (1976); J. Non-Cryst. Solids 31, 157 (1978).
[12]J. Farges, B. Raoult and G. Torchet, J. Chem. Phys. 59, 3454 (1973).
[13]O. Echt, K. Sattler, and E. Recknegel, Phys. Rev. Lett. 47, 1121 (1981).
[14]C. S. Cargill, Ann. N.Y. Acad. Sci. 279, 208 (1976).
[15]P. Steinhardt, D. R. Nelson, and M. Ronchetti, Phys. Rev. Lett. 47, 1297 (1981).
[16]D. R. Nelson and J. Toner, Phys. Rev. B 24, 363 (1981).
[17]For a review, see R. Cotterill, in *Ordering in Strongly Fluctuating Condensed Matter Systems,* edited by T. Riste (Plenum, New York, 1980).
[18]J. Toner (unpublished).
[19]S. Hess, Z. Naturforsch. 359, 69 (1980).
[20]A. C. Mitus and A. Z. Patshinkiii, Zh. Eksp. Teor. Fiz. 80, 1554 (1981) [Sov. Phys.—JETP 53, 798 (1981)]; Phys. Lett. 87A, 179 (1982).
[21]L. D. Landau and F. M. Lifshitz, *Quantum Mechanics* (Pergamon, New York, 1965).
[22]A. D. J. Haymet, Phys. Rev. B 27, 1725 (1983).
[23]G. A. Angell, J. H. R. Clark, and L. V. Woodcock, in *Advances in Chemical Physics,* edited by I. Prigogine and S. A. Rice (Wiley, New York, 1981), Vol. 48.
[24]J. L. Finney, Proc. R. Soc. London Ser. A 319, 479 (1970).
[25]J. D. Bernal, Proc. R. Soc. London Ser. A 280, 299 (1964); see, in particular, Figs. 12 and 13.
[26]Long-range hexatic orientational order does appear in the "stacked hexatic" phase of the smectic liquid-crystal compound 650 B.C. See Ref. 5 and R. Pindak, D. E. Moncton, S. C. Davey, and J. W. Goodby, Phys. Rev. Lett. 44, 1461 (1980).
[27]R. Alben, G. S. Cargill II, and J. Wengel, Phys. Rev. B 13, 835 (1976). See, in particular, their Fig. 2(b). See also, P. Chaudhari and J. F. Graczyk, in *Amorphous and Liquid Semiconductors,* edited by J. Stake and W. Bronig (Taylor and Francis, London, 1974); J. F. Graczyk and P. Chaudhari, Phys. Status. Solidi B 75, 593 (1976).
[28]N. A. Clark, B. J. Ackerson, and A. J. Hurd, Phys. Rev. Lett. 50, 1459 (1983).
[29]H. M. Lindsay and P. M. Chaikin, J. Chem. Phys. 76, 3774 (1982).
[30]D. Turnbull and B. C. Bagley, in *Treatise on Solid State Chemistry,* edited by N. B. Hannay (Plenum, New York, 1975), Vol. 5.
[31]R. Collins, in *Phase Transitions and Critical Phenomena,* edited by C. Domb and M. S. Green (Academic, New York, 1972), Vol. 2.
[32]G. D. Scott and D. L. Mader, Nature (London) 201, 382 (1964).
[33]N. D. Mermin, private communication.
[34]F. H. Busse, J. Fluid Mech. 72, 67 (1975).
[35]D. H. Sattinger, J. Math. Phys. 19, 1720 (1978).
[36]J. Mathews and R. L. Walker, *Mathematical Methods of Physics* (Benjamin, Reading, 1970).
[37]L. D. Landau and E. M. Lifshitz, *Statistical Physics* (Pergamon, London, 1969), Chap. XIV.
[38]See, e.g., S. Goshen, D. Mukamel, and S. Strikman, Solid State Commun. 9, 649 (1971).
[39]L. D. Landau, Phys. Z. Soviet 11, 26 (1937); see also, *The Collected Papers of L. D. Landau,* edited by D. ter Haar (Gordon and Breach—Pergamon, New York, 1965), p. 193.
[40]G. Baym, H. A. Bethe, and C. Pethick, Nucl. Phys. A 175, 1165 (1971).
[41]S. Alexander and J. P. McTague, Phys. Rev. Lett. 40, 702 (1978).
[42]J.-P. Hansen and I. R. McDonald, *Theory of Simple Liquids* (Academic, New York, 1976).
[43]D. Frenkel and J. P. McTague, Phys. Rev. Lett. 42, 1632 (1979).
[44]M. Kleman and J. F. Sadoc, J. Phys. (Paris) Lett. 40, L569 (1979).
[45]N. D. Mermin, Rev. Mod. Phys. 51, 591 (1979).
[46]See, e.g., *Ill-Condensed Matter—III,* Proceedings of the Les Houches Summer School, 1978, edited by R. Balian, R. Maynard, and G. Toulouse (North-Holland, New York, 1978).